Intracellular dynamics of a focal adhesion protein and its relationship to cell migratory activity: an analysis of PAG3, a novel paxillin-binding ARFGAP protein

A thesis presented to the faculty of
Department of Physiological Sciences, School of Life Science,
The Graduate University for Advanced Studies
in partial fulfillment of the requirements for
the degree of Doctor of Philosophy

by
Akiko Kondo

January 31, 2000
The Graduate University for Advanced Studies
Okazaki, Japan

CONTENTS

ABSTRACT

Paxillin acts as an adapter molecule in integrin signaling. Paxillin is localized to focal contacts, but seems to also exist in a relatively large cytoplasmic pool. Here, we report the identification of a new paxillin-binding protein, PAG3 that is involved in regulation of the subcellular localization of paxillin. PAG3 bound to all paxillin isoforms, and was induced during monocyte maturation, at which time paxillin expression is also increased and integrins are activated. PAG3 was diffusely distributed in the cytoplasm in premature monocytes, but became localized at cell periphery in mature monocytes, a fraction of which then colocalized with paxillin. PAG3, on the other hand, did not accumulate at focal adhesion plaques, suggesting that PAG3 is not an integrin assemble protein. PAG3 was identical to KIAA0400/PAPα, which was previously identified as a Pyk2-binding protein bearing a GTPase-activating protein (GAP) activity towards several ARFs in vitro. Mammalian ARFs fall into three classes, and we showed that all classes could affect subcellular localization of paxillin. We also examined possible interaction of PAG3 with ARFs, and showed evidence that at least one of them, ARF6, seems to be an intracellular substrate for GAP activity of PAG3. Moreover, overexpression of PAG3, but not its GAP-inactive mutant, inhibited paxillin recruitment to focal contacts, and hampered cell migratory activities while cell adhesion activities were almost unaffected. Therefore, our results demonstrate that paxillin recruitment to focal adhesions is not mediated by simple cytoplasmic diffusion; rather, PAG3 appears to be involved in this process, possibly through its GAP activity towards ARF proteins. Our result thus delineates a new aspect of regulation of cell migratory activities.

ABBREVIATIONS

AlF, Aluminum fluoride

ARF, ADP-ribosylation factor

BFA, brefeldin A

ECM, extracellular matrix

EGFP, enhanced green fluorescent protein

GAP, GTPase-activating protein

G protein, guanine-nucleotide-binding protein

GST, glutathione S-transferase

HA, influenza hemagglutinin

PAG, Paxillin-associated protein with ARF GAP activity

PCR, polymerase chain reaction

PH, pleckstrin homology

PLD, phospholipase D

SH3, Src homology 3

INTRODUCTION

Cell migration plays essential roles in a wide variety of physiological and pathological aspects of the organization of multicellular organisms, such as embryogenesis, organogenesis, wound repair, inflammatory processes, and cancer invasion and metastasis.

Cell migration, which is primarily mediated by the integrin binding to the extracellular environments or to the extracellular matrixes (ECMs), has been shown to consist of multiple steps; as described, for example, during would healing of fibroblasts and vascular endothelial cells: (1) Membrane extension or protrusion, including both filopodia and lamellipodia, is taken place at front areas of the migrating cells. Membrane extension seems to be mediated by the actin cytoskeletal reorganization. (2) Adhesive complexes are then formed, which is stabilized through the integrin-binding to the extracellular environments. (3) The integrin binding is tightly coupled with the generation of intracellular contractile force as well as the traction force, that are essential for the translocation of the cell body. (4) Generation of intracellular forces is also tightly related to the cell polarity. Through these multiple steps, the small nascent adhesive complexes (focal complexes) formed at the cell front edges seems to grow as cells move forwards, which finally form well-organized focal adhesions and then serve as points of traction over which the body of the cell moves (see Fig. 1).

Integrin family of transmembrane adhesion receptors link cytoplasmic actin-based cytoskeleton to extracellular environments or to the ECMs (reviewed in Hynes, 1992; Lauffenburger and Horwitz, 1996; Sheetz et al., 1998) (see Fig. 2). Intracellular contractile force, which is essential for the cell translocation, is generated by the actin-based cytoskeletal architecture, in which the activities of the Rho-family small guanosine triphosphatases (GTPases), Rho, Rac, and Cdc42, has been shown to play pivotal roles. Moreover, recent studies have revealed that another family of the small GTPases, ARFs (ADP-ribosylation factors), are also deeply involved in these processes.

Properties of several essential molecules involving in the regulation of the cell migration and our study described here are summarized herein.

Integrin

Integrins are the transmembrane cell surface receptors that mediate cell adhesions to extracellular environments. Integrin are composed of α and β heterodimer transmembrane subunits, each consist of 17 isoforms for the α and 8 isoforms for the β. As a consequence of different combination of both isoforms, more than 20 different integrin α and β complexes have been reported. The cytoplasmic domains the α and β isoforms do not possess any intrinsic enzymatic activities. Integrins thus recruit a characteristic set of cytoplasmic proteins, with scaffolding as well as catalytic signaling properties, at their cytoplasmic regions to exert the function (Clark and Brugge, 1995; Burridge and Chrzanowska-Wodnicka, 1996). It is well documented in fibroblasts that integrin macroaggregates grow and shrink in size, density, and shape over time during cell migration, though the position of each macroaggregate remains fixed as the cell translocates (Regen and Horwitz, 1992). It is believed that there must be mechanisms that orchestrate the dynamics of protein recruitment and assembly at the cytoplasmic tails of integrins, but the molecular processes remain to be established (Burridge and Chrzanowska-Wodnicka, 1996). The precise subcellular locations where integrins initially assemble with their cytoplasmic binding proteins are also not known.

The Rho-family of the small GTP-binding proteins (Rho/Rac/Cdc42):

The Rho-family of the small GTP-binding proteins have been shown to be involved in the regulation of actin cytoskeleton organization and focal adhesion formation.

Rho acts as a molecular switch to control a signal transduction pathway that links membrane receptors to the cytoskeleton. Rac, the next member of the Rho family to be analyzed, could be activated by a distinct set of agonists, leading to the assembly of a meshwork of actin filaments at the cell periphery to produce lamellipodia and membrane ruffles. Cdc42, the third member of the Rho subfamily, was shown to induce actin-rich surface protrusions, called filopodia. As with Rho, the cytoskeletal changes induced by Rac and Cdc42 are also associated with distinct, integrin-based adhesion complex formation. Furthermore, in fibroblasts the activities of these three proteins are linked to each other in a hierarchical fashion: Cdc42 can rapidly activate Rac, leading to the intimate association of filopodia and lamellipodia, while Rac can activate Rho, leading potentially to the formation of new sites of focal adhesions and contractile filament assembly within an advancing lamellipodium (Nobes and Hall, 1995).

Ridley and Hall (1992) analyzed early changes in actin organization following the stimulation of quiescent serum-starved Swiss 3T3 cells by a variety of growth factors and observed two major types of alteration. One is that the assembly of new stress fibers accompanied by the formation of focal adhesions (Ridley and Hall, 1992). Another is that an increase in polymerized actin at the plasma membrane forming membrane ruffles. Also, by selectively inhibiting Rho proteins in cells, they showed that Rho is required specifically for the formation of focal adhesions and stress fibers, but not for membrane ruffles. Thus, Rho A has been shown to be involved in the formation of actin stress fibers and focal adhesion assembly in Swiss 3T3 cells. Furthermore, Chrzanowska-Wodnicka and Burridge (1996) showed that Rho A protein has been shown to participate in regulation of the phosphorylation status of myosin light chain (MLC), and thus regulate the contractility of the actomyosin network, using several inhibitors, which are KT5926, Butanedione-2-monoxime (BDM) and 1-(5-isoquinolinylsulfonyl)-2-methylpiperazine (H7), of actin-myosin interaction with distinct modes action to block LPA-induced contractility of Balb/c 3T3 cells (for reviews see Burridge and Chrzanowska-Wodnicka, 1996; Lauffenburger and Horwitz, 1996). KT5926, BDM and H7 is an inhibitor of myosin light chain kinase (MLCK), muscle myosin ATPase activity and protein kinase C (PKC), respectively. The myosin-binding subunit

of myosin light-chan (MLC) phosphatase is a substrate for Rho kinase in vitro. Rho activates Rho kinase, which in turn inhibits the myosin phospatase, thus maintaining MLCs in a highly phosphorylated state. Phosphorylation of myosin-binding subunit lead to a decrease in MLC phosphatase activity, resulting in an accumulation of that phosphorylated (Horwitz and Parsons, 1999)

Chong (1994) et al. also showed that in both intact mouse fibroblasts and in cell lysates, Rho could be to activate phosphatidylinositol 4-phosphate 5-kinase to produce phosphatidylinositol 4, 5-bisphosphate, which interacts with gelsolin, profilin, and vinculin; and helps to regulate actin polymerization and cytoskeleton-membrane attachment (for a review see Burridge and Chrzanowska-Wodnicka, 1996).

Rho is moreover able to activate phospholipase D (PLD) to produce phosphatidic acid, and to regulate actin polymerization (Ha et al., 1994). In neutrophils, Olson et al. (1991) showed that the ability of GTPγS to activated PLD depended on factors in both the cytosolic and plasma membrane fractions, and importantly, a GDP dissociation inhibitor that is specific for Rho family G proteins (Rho GDI) inhibited the stimulation of PLD by GTPγS (Olson et al., 1991). The domain of rPLD1 at which RhoA interacts is located at the C-terminus. The PLD interaction site in RhoA is in the activation loop (Switch I), which is one of the regions that undergo the greatest conformational changes during activation and has the specific residues (Tyr34, Thr37, Phe39 and Thy42) involved by other Rho effectors.

In spite of these extensive studies, however, the precise mechanism of how Rho A, as well as other Rho-family proteins, regulates focal adhesion assembly and its connection to actin fibers that ultimately leads to the regulation of cell migratory activity, remains to be established.

The ARF family of the small GTP-binding proteins:

ARF was originally discovered as a cofactor regulatory subunit (Gas) of adenylate cyclase by cholera toxin. ARF is an abundant protein, comprising nearly 1% of soluble cytosolic protein in at least some neural tissues. The ARF family comprises a group of structurally and functionally conserved proteins of approximately 21 kDa, which belong to members of the Ras superfamily of small GTP-binding proteins. The ARF family is divided functionally into the ARF, and ARF-like (ARL) proteins which do not activate cholera toxin (Tsuchiya et al., 1991; Clark et al., 1993).

Like other small GTP-binding proteins, ARF are active when bound to GTP. However, ARF have three biochemical properties that distinguish them from other GTP-binding proteins: (1) GTP binding is highly dependent on phospholipids; (2) the activated protein, ARF-GTP, associates more stably with phospholipid micelles or membranes, while ARF-GDP is soluble; and (3) purified ARF proteins show no detectable intrinsic GTPase activity in vitro (<0.0015 min-1).

ARF isoforms share more than 60% sequence identity, and express ubiquitous in eukaryotes and highly conserved throughout evolution; for example, human, *Drosophila melanogaster* and *Schizosaccharomyces pombe* arf1 share more than 90% identity. There are three ARF genes in *S. cerevisiae* and six in mammals. Mammalian six ARF isoforms are highly homologous to one another, and classified as class I, II or III based of on the size and the amino acid identity (Tsuchiya et al., 1991). Class I includes ARF1, 2 and 3 (181 amino acids); class II, ARF4 and 5 (180 amino acids); and class III, ARF6 (175 amino acids). Among them, ARF1 has been most thoroughly studied. ARF1 and ARF6 isoforms, which are closely involved in our study, are described below in some more details.

ARF1

ARF1 has been shown to regulate membrane traffic at multiple sites within the cell. A

secretion-defective phenotype associated with ARF mutants in the yeast *S. cerevisiae*, synthetic lethality observed when viable ARF mutants and combined with a specific subset of SEC genes (Stearns et al., 1990). The first clue to its physiological role in the cell was immunofluorescence and immunocytochemistry data showing that ARF is concentrated in the Golgi apparatus. The ability of peptides corresponding to the N-terminus of ARF to inhibit in vitro transport reactions has implicated ARF in endoplasmic reticulum (ER) to Golgi transport, endosome-endosome fusion, protein secretion and fluid-phase endocytosis, as well as in transport between Golgi cisternae (Rothman and Wieland, 1996; Schekman and Orci, 1996).

A fungous macrocyclic lactone, Brefeldin A (BFA), inhibits several ARF exchange factors and prevents ARF1 membrane binding in vitro, and thus causes the rapid release of coat proteins, including b-COP, from Golgi into the cytosol or ER (reviewed in Chardin and McCormick, 1999). ARF1 also is an activator of PLD and can regulate vesicle budding from the TGN by modulating PLD activity.

The GTP bound form of ARF1 recruits protein coats, including the clathrin-associated adapter proteins AP-1 and AP-3, and the non-clathrin coatomer COPI, to membranes and initiates budding of the membrane vesicles (Roth et al., 1997). AP-1 plays a role in protein sorting from the TGN and endosome to compartments of the endosomal / lysosomal system. AP-2 is contained in clathrin-coated vesicles forming from the plasma membrane (Chen et al., 1998; Hussain et al., 1999). AP3- is associated with endosomes and/or the TGN and recruits internal membrane proteins for to lysosomes and lysosome-related organelles. Recently, AP-4 was reported (Dell'Angelica et al., 1999). AP-4 was found to localize to TGN or a neighboring compartment. AP-1, AP-3 and AP-4 are sensitive proteins to Brefeldin A, a drug that affects the subcellular distribution. ARF1 T31N, which is ARF1 dominant-negative mutant, renders endogenous ARF1 inactive, presumably by binding to and sequestering an ARF1 guanine nucleotide exchange factor (ARF GEF), and produces a BFA-like phenotype. In these mutant transfected cells, AP1 and AP-3 distribution was no longer punctate but appeared cytosolic, reminiscent of the effect of BFA, whereas AP-2 distribution was not affected. ARF1 Q71L, which is a constitutively active ARF1

mutant, protects coatomer from BFA-induced membrane dissociation. The COPI-coated vesicles formation, a preassembled complex of seven subunits (α-, β-, β '-, γ-, δ-, ε-, ζ-COP), involves a direct interaction with membrane-bound ARF1-GTP and coatomer via its β-COP and γ-COP. Subsequent hydrolysis of GTP to GDP by ARF1 may trigger disassembly of the coat from the vesicle, which is necessary for the vesicle to fuse to the target membranes.

ARF6

ARF6, the ARF that is most distantly related to ARF1, shows a rather wide distribution in the cytoplasm and localizes to an endosomal compartment and membrane ruffling regions (Peter et al., 1995). Brefeldin A (BFA) has no effect on ARF6 (Peter et al., 1995; Cavenagh et al., 1996; Radhakrishna et al., 1996). ARF6 primarily regulates endosomal trafficking as well as receptor-mediated endocytosis at the cell periphery, actin rearrangements beneath the plasma membrane, and cell spreading (Peter et al., 1995; D'Souza-Schorey et al., 1995; Radhakrishna et al., 1996; Radhakrishna and Donaldson, 1997; Song et al., 1998; Radhakrishna et al., 1999).

ARF6 localizes to an endosomal compartment in the GDP state and to the plasma membrane in the GTP state. Activation of ARF6, through nucleotide exchange, triggers membrane recycling from this endosomal compartment to the plasma membrane. This recycling is blocked in cells treated with cytochalasin D or in cells expressing the GTP-binding defective mutant ARF6 T27N (Radhakrishna et al., 1997; D'Souza-Schorey et al., 1998). ARF6 T27N predicted to be defective in GTP binding and hence predominantly in the inactive, GDP sate, is associated almost exclusively with the internal endosome-like structures. Another mutant of ARF, ARF6 Q67N, predicted to be defective in GTP hydrolysis, and thus predominantly in the active, GTP sate, in confined to the plasma membrane. ARF6 Q67N transfected cells results in the formation of peripheral plasma membrane protrusions (Radhakrishna et al., 1996; D'Souza-Schorey et al., 1997).

Radhakrishna et al. (1996) showed that in transiently wild-type ARF6 transfected HeLa cells,

these membrane protrusions also induced with the G-protein activator aluminum fluoride (AlF). Recent studies suggest that ARF6-regulated membrane recycling in critical for initiating changes in cortical actin architecture. Whether Rho proteins are required for the ARF6 cortical actin changes and whether ARf6 is required for Rho-induced changes, however, is known.

Furthermore, it was reported that ARF6 and Rac1 bind to a common protein required for stimulation of actin rearrangement, POR1 (partner of Rac1; D'Shouza Schorey et al., 1997) In macrophages, it has been reported that normal guanine nucleotide cycling on ARF6 was required for Fcγ-R mediated phagocytosis (Zhang et al., 1998). Inhibition of either Rac1 or ARF6 function produced the same phenotype in macrophages challenged with immunoglobulin G-coated particles. ARF6 and Rac1 may lie on the same pathway leading to cytoskeletal alterations and pseudopodial formation.

Integrin-assembly Proteins:

Integrin requires an assembly of a number of proteins at their cytoplasmic tails to exert the function. Among them, we focus on paxillin in this study. The rationale of our use of paxillin will be described later.

Paxillin

Paxillin is highly tyrosine phosphorylated upon integrin activation and acts as an adapter protein in integrin signaling (see Fig. 3).

Paxillin was originally identified as a substrate for the v-Src tyrosine kinase. Paxillin is the 68 kDa adapter protein and can be divided superficially into two distinct structural domains.

The first comprises the amino-terminal 325 amino acids and contains binding sites for vinculin, and the non-receptor tyrosine kinases focal adhesion kinase (FAK) and the FAK-related kinase, PYK2. Careful analysis of these binding sites on paxillin revealed that they each contain a novel 8 amino acid repeating sequence which have been named paxillin LD motifs because of the invariant leucine-aspartate pairing of amino acids that begin the repeat. These motifs, in turn, interact with common paxillin binding subdomains (PBS) within vinculin and FAK. The amino terminal half of paxillin also contains proline-rich domains that interact with the SH3 domains of Src and Crk family members and contains binding sites, including the SH2-binding motifs, that are available for interaction with their ligand only when they are phosphorylated. The carboxyl-terminus (amino acids 326-559) of paxillin is composed exclusively of four LIM domains. These are double zinc finger motifs, each of approximately 50 amino acids. LIM domains are found in a wide variety of proteins including transcription factors as well as cytoskeleton-associated molecules. In general, they serve as another protein-protein binding module. In the case of paxillin, the third LIM domain is absolutely essential for targeting the protein to focal adhesion via this domain remains to be determined. Paxillin has been implicated in the regulation of focal adhesion assembly and signal transduction through these tyrosine phosphorylated in response to cell adhesion to ECM and following challenge of serum-starved cells with soluble growth factors (Burridge et al., 1992; Zachary et al., 1993; Rozengurt, 1995). Recent reports indicate that serine/threonine phosphorylation of paxillin also occurs in response to adhesion of cells to ECM and that, as with FAK, the serine/threonine kinases are physically associated with paxillin (DeNichoilo and Yamada, 1996; Bellis et al., 1997; Brown et al., 1998). It has been reported that human has multiple isoforms paxillin α, β and γ, whereas rodent has paxillin α and β isoform but not γ (Mazaki et al., 1997). Human paxillin isoforms is different biochemical properties and different patterns of expression. Paxillin α has been shown to bind to Fak, talin, and vinculin. On the other hand, paxillin β has been shown to bind to Fak and talin similarly but exhibits only marginal binding to vinculin; isoform γ has been shown to bind to vinculin and talin similarly but only weakly binds to Fak. Paxillin α has expressed ubiquitously in most normal tissues. Paxillin β and γ, on the other

hands, have been shown to be expressed in a certain types of cells including monocytes and cancer cells (Mazaki et al., 1997).

It has been believed there are mechanisms that regulate and orchestrate the intracellular dynamics of integrin-assembly proteins. These putative mechanisms may play important roles in the dynamic aspects of integrin function including cell migration. In this study, we analyzed the intracellular dynamics of paxillin.

We found that paxillin in fibroblastic cells is highly localized at the perinuclear areas largely overlapped with the Golgi apparatus, in addition to its localization to the focal adhesions. Paxillin is a soluble protein biochemically; thus some factor(s) may be involved in this perinuclear localization. We have also shown that some organelle structure seems to be involved in this perinuclear localization of paxillin (will be described later). Moreover, recent studies by Norman et al. have shown that ADP-ribosylation factor 1 (ARF1) participates in paxillin recruitment to sites of focal contacts in Swiss 3T3 (Norman et al., 1998). We thus hypothesized that some active cellular process regulates the subcellular localization as well as the intracellular dynamics of paxillin. Elucidation of the perinuclear localization of paxillin may contribute to the understanding of its intracellular dynamics, which is closely related to the focal adhesion formation during cell migration. We attempted to identify the putative paxillin binding protein(s) that is thereby involved intracellular dynamics of paxillin.

For this purpose, we used monocyte cells. The process of monocyte maturation in vitro

provides a good model to explore the biochemical events involved in process of integrin activation. Human monocytes express all three isoforms of paxillin, and expression of all isoforms is augmented upon the cell maturation. Here, we report the isolation of a paxillin-binding protein, named PAG3 (Paxillin-associated protein with ARF GTPase-activating protein (GAP) activity, number 3), from mature U937 monocyte cells. PAG3 corresponds to KIAA0400 previously isolated from human brain by Ishikawa et al., 1997; and during my analysis, the same molecule was also identified as a Pyk2 (Proline-rich tyrosine kinase 2) binding protein, which is a s member of the FAK nonreceptor tyrosine kinase family, and named Papa (Pyk2 C terminus-associated protein). PAG3/Papa/KIAA0400 contains a zinc finger motif that is highly homologous to that of mammalian ARF1 GAP (purified from rat liver cytosol) and yeast ARF GAP protein Gcs1. The zinc finger motif, a conserved CxxC-x16-CxxC motif (where x is any amino acid), is essential for the ARF1 GAP activity. Andreev et al. have shown that this protein exhibits a GAP activity against several isoforms of ARFs in vitro; and also demonstrated that this protein inhibits ARF-dependent generation of post-Golgi vesicles and secretion of a truncated form of placental alkaline phosphatase. We show here that PAG3/Papα/KIAA0400 also binds to all three isoforms of human paxillin (α, β and γ), and is highly induced during monocyte maturation, during which integrins are activated and the cells become adherent and motile. We analyzed intracellular interactions among paxillin, PAG3 and ARFs. We also suggest that the GAP activity of PAG3 is involved in the recruitment of paxillin to focal contacts of adhesion plaques, and cell migratory activity. Finally, we discuss the relationship of ARF-mediated intracellular regulations to the subcellular localization of paxillin, and to cell migratory activities.

MATERIALS AND METHODS

Cells culture

COS-7 (monkey kidney) cells were grown with DMEM (with 4.5 g glucose /l) (Gibco BRL, Gaitherburg, MD) supplemented with 10% FCS (Hyclone Laboratories, Inc., Logan, UT). HeLa (human epithelial) cells and 293T (human kidney) cells were cultured with DMEM supplemented with 10%FCS (Gibco BRL).

U937 (human peripheral monocytes) cells were cultured with RPMI 1640 with 10% FCS (Gibco BRL). Human peripheral monocytes were prepared from peripheral venous blood collected from normal donors. Monocyte cells in the blood sample were isolated by centrifugation on Ficoll-Paque Plus (Pharmacia Biotech, Uppsala, Sweden) followed by sedimentation through Percoll (Pharmacia Biotech) according to the manufacturer's instructions, and cultured with RPMI 1640 supplemented with 10% FCS. For differentiation, monocyte cells were treated with 1.6 X 10 -7 M 12-O-tetradecanoyl-phorbol acetate (TPA; Sigma Chemical, St. Louis, MO) for three days (Gidlund et al., 1981).

NMuMG cells (CRL 1639) with a passage number of 15 were obtained from American Type Culture Collection [ATCC] (Rockville, MD) and grown in DMEM (with 4.5 g glucose/l) supplemented with 10% FCS (Hyclone Laboratories, Inc., Logan, UT), 10 μg/ml insulin (Gibco BRL, Rockville, MD), 100 μg/ml penicillin, and 100 U/ml streptomycin at 37 oC in 5% CO2. After the initial expansion for three days cells were frozen in aliquots; and in each experiment, cells were cultured no longer than two weeks by subculturing at a dilution of 1 : 10 - 1 : 20 every third day following 0.25% trypsin-EDTA treatment. Trypsinization was done for 10 min at ambient temperature. For transdifferentiation into the mesenchymal phenotype, 8 x 105 NMuMG cells were seeded in a 9 cm culture dish (Beckton Dickenson, Franklin Lakes NJ), and 24 h later 2 ng/ml TGF β1 (R & D Systems, Minneapolis MN) was added, and cells were cultured further for 48h as

described before (Miettinen et al., 1994), unless otherwise indicated. For analysis of the epithelial phenotype, 8 x 105 cells were seeded in a 9 cm culture dish and cultured for three days. Parental NMuMG cells, both in epithelial and mesenchymal forms, reached confluence under these conditions. To examine cells under sparse culture conditions, 2 x 105 cells were seeded initially and then processed as above. Under these conditions, apparent cell confluence is less than 20% in both the epithelial and mesenchymal phenotypes.

PC12 (Rat pheochromocytoma) cells were grown with DMEM (Gibco BRL, Gaitherburg, MD) supplemented with 10% FCS and 10% HS.

Antibodies

Anti-paxillin antibody (Ab199-217), which recognizes the α, β and γ isoforms, was described previously (Mazaki et al., 1997).

Rabbit polyclonal anti-PAG3 antisera was raised against glutathione S-transferase (GST)-fusion forms of PAG3 (M2) protein produced in *E. coli* (see below), which contained amino acids 863 to 1006 of PAG3. The antisera was affinity-purified using GST-PAG3 (M2) protein before use.

Other antibodies were purchased from commercial sources: anti-paxillin (mouse monoclonal, Transduction Laboratories, Lexington, KY), anti-influenza hemagglutinin (HA) (clone 16B12; Berkeley Antibody Co., Richmond, CA), anti-green fluorescent protein (GFP) (Clontech, Palo Alto, CA), anti-Pyk2 (mouse monoclonal, Transduction Laboratories), anti-phosphotyrosine (4G10; Upstate Biotechnology Inc., Lake Placid, NY). Anti-β-COP antibody were gifts from Dr. M. Tagaya (Tokyo University of Pharmacy and Life Science, Hachioji,Tokyo, Japan).

Secondary antibodies to rabbit or mouse IgG each conjugated with peroxidase, Cy2, and Cy5 were from Jackson ImmunoResearch Laboratories (West Grove, PA).

Plasmids and Recombinant Proteins

All procedures for nucleic acid manipulation were done according to standard methods (Sambrook et al., 1989) unless otherwise described.

pAcG2TK/paxillin a was constructed by ligating the Bam HI-Eco RI cDNA fragment isolated from pGEX/paxillin a (Mazaki et al., 1997), encoding the entire region of human paxillin α, into the Bam HI-Eco RI site of pGEX-2TK (Pharmacia Biotech) to be fused in frame to the COOH-terminus of GST. The recombinant protein produced in *E. coli* by the induction with isopropyl-β-D-thiogalactopyranoside was purified using glutathione-Sepharose beads (Pharmacia Biotech), and phosphorylated in vitro using catalytic subunit of cAMP-dependent kinase (Sigma Chemical, St. Louis, MO) and [γ-32P] ATP according to a method previously described (Kaelin et al., 1992). TPA-induced monocyte U937 λgt 11 cDNA library (Clontech) was then screened using the phosphorylated GST-TK-paxillin a protein as a probe.

KIAA0400 cDNA was a gift from Dr. T. Nagase at Kazusa DNA Research Institute (Chiba, Japan). The cDNA fragment was amplified by a polymerase chain reaction (PCR) method using oligonucleotides; 5'-GCT GAA GGT CAA CGA AAT CA-3' and 5'-TGC TAT TTT GCA GCA CAG AC-3', and the resultant fragment was ligated into the Bam HI-Not I site of pEBG expression vector (Mayer et al., 1995) to be fused in frame to the COOH-terminus of GST.

For construction of mutants of PAG3 cDNA, each corresponding cDNA fragment was amplified from the original KIAA0400 cDNA by PCR and ligated into the pGEX-2TK (for M1 and M2 mutants) or pEBG (M3 and M4 mutants) vectors in frame with the COOH-terminus of GST. Production of the M3 and M4 mutants in E. coli was accompanied by severe degradation of the

recombinant proteins, thus the mammalian expression system was used for these proteins. Oligonucleotides used were as follows, 5'-CGGGATCCGCGCTCTATAACTGTGTGGCTGACA-3' and 5'-CGGGATCCTCAGTCAGCGATAAAGTGCACAAAT-3' for M1 mutant encompassing the amino acids 951 to 1006 (951-1006 aa); 5'-CGGGATCCCCGAGCAAGCCTGCCCCGCC-3' and 5'-CGGAATTCTCAGTCAGCGATAAAGTGCA-3' for M2 (863-1006 aa); 5'-CGGGATCC GTTCACGTTGAATATGAATGGCGAC-3' and 5'-AAGGAAAAAAGCGGCCGCTCAGTCAGCGATAAAGTGCAC-3' for M3(685-1006 aa); 5'-CGGGATCCATGCCGGACCAGATCTCCG T-3' and 5'-AAGGAAAAAAGCGGCCGCTCAGTGAGAATTAAATCTTCCAGATAA G-3' for M4(1-684 aa). Proteins encoded by the pGEX2TK vector were produced in E. coli by induction with isopropyl-β-D-thiogalactopyranoside, and proteins encoded by the pEBG vector were produced in COS-7 cells. These proteins were then subjected to purification using glutathione beads as previously described (Mazaki et al., 1997).

EGFP fusion protein with PAG3 was made by isolating the Sma I-Sma I cDNA fragment from pGEX2TK/PAG3 containing the entire region of PAG3 and ligating it into the Sma I site of the pEGFP-C1 vector (Clontech), fusing it in frame with the COOH-terminus of EGFP. For the construction of C436A mutant of PAG3 (CA mutant) in which the critical cysteine residue for the GAP activity at amino acid 436 was mutated into alanine to diminish the GAP activity as in the case of ARF1 GAP (Cukierman et al., 1995), the 680 bp Aat II-Stu I fragment corresponding to that of the original cDNA but encoding the mutation was made by PCR using 5 ' - GGCAATGACGTCGCCTGTGACTGTGGGGCG-3 ' and 5 ' - AAAAGGCCTTCCCCCGCAGGAGCAACTTGA G-3]. The Aat II-Stu I fragment of the pEGFP-C1/PAG3 was then replaced with the resulting fragment.

Recombinant proteins were made in the baculovirus system by ligating Bgl II-Eco RI cDNA fragments each encoding the entire coding region of human paxillin α, β and γ isolated from

pBabePuro/paxillin plasmids (Mazaki et al., 1997) into the Bgl II-Eco RI site of the pVL1392 vector (Pharmingen, San Diego, CA). pAcG2T/Paxillin α (N) and pAcG2T/Paxillin (LIM), each encoding a GST-fusion protein with the N-terminal half of paxillin a (1-324 aa) and the four repeats of paxillin LIM domains (325-557 aa) were constructed by ligating each cDNA fragment amplified from pGEX2T/paxillin α (Mazaki et al., 1997) using oligonucleotides of 5'-ATGGATCCATGGACGACCTCGACGCCCTGCTG-3' and 5'-ATGAATTCCTGCAGAGTCCGCGACTGTGGCG-3', and 5'-ATGGATCCGGGGCCTGCAAGAAGCCCATCGC-3' and 5'-ATGAATTCCTAGCAGAAGAGCTTGAGGAAGC-3', into the Bam HI-Eco RI site of pAcG2T baculovirus vector. Each recombinant protein was produced according to the manufacturer's instructions (Pharmingen).

cDNAs in pcDNA 3 vector each encoding HA-ARF1, HA-ARF5, HA-ARF6, HA-ARF1 N126I, HA-ARF5 N126I and HA-ARF6 N122I were gifts from Dr. K. Nakayama (Tsukuba University, Tsukuba, Ibaraki, Japan).

Nucleotide sequences were confirmed with all the plasmids after the construction.

Protein Binding Analysis

Cell lysates were prepared with 1% NP-40 buffer [1% Nonidet P-40, 150 mM NaCl, 20 mM Tris-HCl (pH 7.4), 5 mM EDTA, 1mM Na3VO4, 1 mM PMSF, 1% aprotinin, 2 mg/ml leupeptin and 3 mg/ml pepstatin A] as described previously (Sabe et al., 1994). Protein concentrations were determined using a Dc protein assay kit (Bio-Rad, Lab., Hercules, CA) with BSA (Sigma) as a standard.

For radiolabeling, HeLa cells were incubated in the presence of 0.1 mCi/ml L-[4, 5-3H] leucine (80 Ci/mmol, Moravek Biochemikals) in Dulbecco's modified Eagle's medium (without L-

leucine, Life Technologies, Inc.) containing 10% dialyzed FCS for 7 h, after being starved for L-leucine by incubating in Dulbecco's modified Eagle's medium (without L-leucine) with 10% dialyzed FCS for 30 min.

For protein binding analysis, 500 mg of cell lysate was mixed with 5 mg of GST-fusion protein bound to glutathione-beads, unless otherwise mentioned, incubated for 1 h at 4 oC, and then washed four times with 1% NP-40 buffer. Proteins retained on the beads were then separated by SDS-PAGE and subjected to immunoblotting analysis visualized by an enzyme-linked chemiluminescence method, as previously described (Sabe et al., 1994; Mazaki et al., 1998).

In the case of radiolabeled cell lysates, protein recovered with the beads was resolved by 8% SDS-PAGE. Gels were fixed in isopropanol:water:acetic acid (25:65:10) solution, soked in Amplify solution (Amersham), and then dried and subjected to fluorography. Prestained rainbow markers (Amersham) were used as size standards.

mRNA Expression Analysis

For detection of mRNA expression of PAG3, premade Northern blots of polyadenylated RNA (Multiple Tissue Northern Blots, Human 12-Lane#7780-1, Clontech) were used. Northern blotting analyses were done using a PAG3 DNA fragment of approximately 1kb.
A probe DNA fragment was synthesized by PCR amplification of each cDNA of PAG3, using oligonucleotides of 5 ' -CTGGCTCACGTGGAAAATGA-3 ' and 5'-TGCTATTTTGCAGCACAGAC-3'. A probe for β-actin (Clontech) was used as a standard control.

Protein Transient Expressions and Confocal Immunofluorescence Microscopy

0.5-1 x 105 COS-7 cells in a 35 mm culture dish were transfected with 4 mg of plasmid DNAs by the calcium phosphate precipitation method as previously described (Bonifacino et al., 1989), or with 1 mg of plasmid DNAs using FuGENE 6 according to the manufacturer's instructions (Boheringer-Mannheim, Indianapolis, IN), and 16-20 h later cells were trypsinized and replated onto glass chamber slides (Polystyrene Vessel Tissue Culture Treated Glass Slide; Becton Dickinson, San Jose, CA). 36-48 h after transfection, cells were fixed in 3.7% paraformaldehyde (Sigma) in PBS for 10 min at room temperature, washed twice with PBS, and then incubated for 5 min in 0.1% BSA/PBS. To activate GTP-binding proteins, cells were treated for 1 h with 30 mM NaF and 50 mM AlCl3 (AlF) at 37 oC as previously described (Radhakrishna et al., 1996; Ooi et al., 1998), before fixation. 1 h incubation with AlF was chosen by our preliminary time-course study (from 10 min to 120 min), as optimal for activation of transfected ARFs in COS-7 cells. Cells were then subjected to successive incubations with primary and secondary antibodies in the presence of 0.2% saponin (Sigma) and 0.1% BSA/PBS. For observation of adhesion plaques, fixed cells were permeabilized by incubating for 5 min with 0.2% Triton X-100/PBS and successive incubations with primary and secondary antibodies each diluted in 2% BSA/PBS. Incubation with each antibody was carried out at room temperature for 1 h, and samples were rinsed with PBS after each antibody incubation. After a final rinse with PBS, coverslips were mounted with 50% glycerol/PBS. Cells were visualized and confocal images acquired using a confocal laser scanning microscope (model 510; Carl Zeiss, Inc., Oberkochen, Germany). Each figure of microscopic analysis showed representative results that were observed in a majority of the cDNA-transfected cells.

Cell Adhesion and Haptotaxis Migration Assays

Cell adhesion and migration assays were performed using modified Boyden chambers

(tissue culture-treated, 6.5-mm diameter, 10 μm thickness, 8-μm pores, Transwell; Costar Corp., Cambridge, MA), as previously described (Klemke et al., 1998). In brief, only the underside of the polycarbonate membrane on the upper chambers was coated with 10 μg/ml of collagen type I (Upstate Biotechnology Inc, Lake Placid, NY), fibronectin (Sigma), vitronectin (Wako Chemicals, Tokyo, Japan) or BSA in PBS for 2 h at 37 oC, rinsed with PBS and then placed into the lower chamber filled with 400 μl of a migration assay medium (fibroblast basal medium supplemented with 0.5% BSA; Clonetics, San. Diego, CA). COS-7 cells (2 x 105 cells / 60 mm-dish) were transfected with each 2.6 μg of pEGFP-C1/PAG3 or pEGFP-C1/PAG3 (CA) using FuGENE 6, and 40 h after transfection cells were trypsinized and washed once with DMEM containing 0.5% (w/v) soybean trypsin inhibitor (Sigma), twice with a migration assay medium and suspended in same medium at 1 x 106 cells/ml. 1 x 105 cells were then applied onto the upper migration chambers, and allowed to migrate into the underside of the upper chamber for 3 h at 37 oC with 5% CO2. After the nonmigrated cells on the upper membrane surface were removed with a cotton swab, cells that migrated to the underside of the upper chamber were fixed with 3.7% paraformaldehyde in PBS. To measure the adhesive activity, another 1 x 105 cells were plated onto culture dishes, which was coated with each ECM and also blocked with heat-inactivated BSA (inactivated at 70 oC for 1 h), incubated for 30 min at 37 oC and then fixed as above. cDNA transfection efficiency was measured by fixing cells without trypsinization. Cells positive for EGFP-PAG3 or EGFP-PAG3 (CA) were detected by fluorescence from the EGFP and counted using a laser scanning microscope with a 20 X objective (model-510, Carl Zeiss). Before data acquisition, the threshold for the detection of the laser scanning microscope was adjusted so as to eliminate the background autofluorescence signals of mock transfected cells. Percent cell adhesion and percent cell migration were calculated by dividing the numbers of transfection-positive adhered cells or migrating cells by the number of applied transfection-positive cells, which was calculated by the cDNA transfection efficiency. Each determination represents the average of three independent experiments, and error bars represent the SEM.

Percent cell adhesion

$$\% = \frac{\text{the numbers of transfection-positive adherenced cells} \times A}{\text{the number of applied transfection-positive cells}}$$

$$= \frac{\text{the numbers of transfection-positive adherenced cells} \times A}{1 \times 10^5 \times \text{0.01 x the cDNA transfection efficiency (\%)}}$$

A = area of well / area of view

area of 48 well (ref. catalog) : 63.6 mm^2

area of ϕ35 mm dish (ref. catalog) : 8.0 cm^2

area of view : calculation in photoshop from 8-μm pore size : 0.49 mm^2

Percent cell migration

$$\% = \frac{\text{the number of transfection-positive migrating cells} \times H}{\text{the number of applied transfection-positive cells}}$$

$$= \frac{\text{the number of transfection-positive migrating cells} \times 67.3}{1 \times 10^5 \times \text{0.01 x the cDNA transfection efficiency (\%)}}$$

H = area of transwell / area of view

area of transwell (ref. catalog) : 0.33 cm^2

area of view : calculation in photoshop from 8-μm pore size : 0.49 mm^2

RESULTS

Isolation of a New Paxillin-Binding Protein PAG3

A λgt 11 cDNA expression library prepared from phorbol-ester stimulated U937 cells was screened by the Far Western protein-blotting method using GST-TK-paxillin α protein as a probe. By screening 5 x 106 plaques, we isolated two cDNA clones (clone 43, clone 81) that strongly bound to the probe. Sequencing analysis revealed that these two clones encoded the same protein, but did not cover the entire coding region of the protein. We then searched a computer database of expressed sequence tags, and found that KIAA0400 cDNA (Ishikawa et al., 1997) and s19 cDNA (Yamabhai and Kay, 1997) showed a close similarity to our clones (Fig. 4). The s19 cDNA clone was identified as a novel protein contained SH3 domain at its C-terminus that interacted with Src SH3 domain and did not contain the entire protein-coding region. KIAA0400 cDNA, on the other hand, contained a complete protein coding region and encoded a protein with 1,006 amino acids, which contained multiple protein modules, including a pleckstrin homology (PH) domain, three repeats of an ankyrin motif, proline-rich sequence and an src homology 3 (SH3) domain. The proline-rich sequence of PAG3 contains several consensus binding sites for SH3 domains (PxxP), including four binding sites for type II SH3 domains (PxxPxR). This protein also contained a zinc finger with a structure of CxxC-x16-CxxC, which showed a close similarity to that of ARF1GAP (Cukierman et al., 1995) (Fig. 5). We had also identified several novel paxillin-binding proteins (our unpublished results), and found that cDNAs corresponding to these paxillin-binding proteins all contained the conserved CxxC-x16-CxxC motif of ARFGAP1 (also see Fig. 5). The primary structure of PAG3 is shown in Fig. 6. We thus named these paxillin-binding proteins PAGs (Paxillin-associated ARFGAP proteins). We call KIAA0400 cDNA as PAG3 (Paxillin-associated ARF GAP protein number 3), and report its analysis here.

During our analysis of PAG3, the same cDNA clone was reported to be identified as a Pyk2-associated protein named PAPα, and has been shown to exhibit GAP activity against ARF1, ARF5 and ARF6 in vitro (Andreev et al., 1999). In this paper, we refer to KIAA0400/PAPα/PAG3 as PAG3 for short.

Binding of PAG3 to paxillin in vitro and in vivo

Binding of PAG3 to paxillin was then confirmed using in vitro and in vivo protein binding assay. We constructed a cDNA encoding GST fused to PAG3 and expressed in COS-7 cells. The recombinant GST-fusion protein was purified on glutathione-beads, and then incubated with each isoform of recombinant paxillin, α, β and γ, produced by the baculovirus system. As shown in Fig. 7, we found that each isoform was equally bound to the GST-PAG3 in vitro.

To examine the in vivo binding of PAG3 and paxillin, COS-7 cells were transfected with GST-PAG3 plasmid, and the GST-fusion protein was pulled-down using glutathione-beads. As shown in Fig. 8, a significant amount of endogenous paxillin was co-precipitated with the beads. Under these conditions, co-precipitation of endogenous p130Cas, Fak and Src was not detected.

Rabbit polyclonal anti-PAG3 antiserum was then raised against GST-fusion forms of the M2 mutant, which corresponds to the amino acids 863 to 1006. To examine the in vivo binding of endogenous PAG3 with the endogenous paxillin, cell lysates prepared from TPA-treated U937 cells were subjected to immunopresipitation using anti-PAG3 antibody (lane 2) coupled with A-Sepharose beads. As shown in Fig. 9, a significant amount of endogenous paxillin was co-precipitated with the antibody beads, as compared to beads with the pre-immune serum (lane 1).

We then dissect the binding regions of paxillin towards PAG3. Paxillin can be divided

into the N-terminal half and the C-terminal four LIM domains. The N-terminal half has been shown to bind to several proteins including tyrosine kinases Src and Fak, and cytoskeleton protein vinculin and talin. LIM domains, in general, have been implicated for protein-protein binding. As shown in Fig. 10, PAG3 bound to the N-terminal half, but not to the LIM domains.

We next constructed a series of deletion mutants of PAG3, and tested their binding towards recombinant paxillin α. As shown in Fig. 11, the C-terminal region of PAG3 contained in the M2 mutant was sufficient for binding; this mutant contained a region similar to our original short cDNA clone (clone 43). The M3 mutant contained the proline-rich sequence and the SH3 domain, which existed proximal to the C-terminus of PAG3. The SH3 domain alone of PAG3 (M1 mutant), however, was not sufficient for binding (Fig. 11, lane 4).

PAG3 binds several different proteins

PAG3 contains several protein-protein interacting motifs; thus paxillin may not be a single protein that bind to PAG3. To explore the potential PAG3-binding proteins, radiolabeled HeLa cell lysates were pulled-down using GST-PAG3. As shown in Fig. 12, we found that at least 7 different protein bands were co-precipitated with GST-PAG3 over those seen with control GST protein. Judging from the molecular sizes, protein band E may correspond to paxillin, and band D may be Pyk2. In addition to these proteins, five bands were detected: A, B, C, F and G.

Protein expression of PAG3

PAG3 protein expression was also detected in several cultured cell lines, including COS-7 (monkey kidney), Vero (monkey kidney), HeLa (human epithelial carcinoma) and U937 (Fig. 13).

Pyk2 protein was detected at marginal levels in Vero, 293T, NIH3T3 and COS-7. Both PAG3 and paxillin expression was increased when U937 monocyte cells were induced to be differentiated by the TPA treatment (Fig. 13). Similar induction of these proteins was also observed during the epithelio-mesenchymal transdifferentiation of NMuMG cells. On the other hand, Pyk2 protein expression was almost unchanged during the monocyte maturation as well as the epithelio-mesenchymal transdifferentiation (Fig. 13).

Expression of PAG3 mRNA in normal human tissues

PAG3 expression in normal human tissues was then examined by Northern blot analysis. Filters containing normal human mRNAs were purchased from the commercial source and hybridized with a 32P-labeled cDNA fragment of PAG3 probe. PAG3 mRNA of approximately 5.7 kb was clearly detected in brain, kidney, and heart; and with relatively low levels in placenta and lung (Fig. 14).

PAG3 is Induced and Binds to Paxillin during Monocyte Maturation

We showed that PAG3 is induced to be expressed during maturation of U937 monocyte cells. Similar induction of PAG3 was also confirmed with monocyte cells when stimulated with TPA, which was prepared from human peripheral blood (Fig. 15, lane 3 and 4). Moreover, we also found that PAG3 became tyrosine phosphorylated during monocyte maturation (Fig. 16).

U937 monocyte cell lysates, GST-PAG3 pulled down both Pyk2 and paxillin. We also found that although binding of PAG3 to Pyk2 was almost unchanged before and after monocyte maturation, binding to paxillin was increased several fold upon monocyte maturation (Fig. 17).

We also tested binding of a series of deletion mutants of GST-PAG3 towards endogenous Pyk2 in U937 cells lysates. As shown in Fig. 18, the C-terminal region of PAG3 contained in the M2 mutant was sufficient for binding (lane 5). We found that both paxillin and Pyk2 bound to the M2 and M3 mutants of PAG3, suggesting that paxillin and Pyk2 may bind to the same region of PAG3 (Fig. 11 and 18).

Colocalization of Endogenous PAG3 and Paxillin at the Cell Periphery

Colocalization of endogenous PAG3 and paxillin was then investigated with U937 monocyte cells (Fig. 19 A). In unstimulated cells, both paxillin and PAG3 showed very weak staining. With TPA-stimulated and adhered cells, significant fractions of both PAG3 and paxillin were detected at the leading edges of the peripheral membrane, and colocalization of both proteins was seen at several, but not all, regions of the cell periphery.

To analyze further the precise subcellular localization of the proteins as well as their intracellular interactions, we employed COS-7 epithelial cells rather than monocyte cells for technical reasons. Moreover, we found that COS-7 cells expressed significant amounts of endogenous PAG3 (see Fig. 13) and paxillin but only marginal levels of Pyk2 (see Fig. 13, lane 9), thus reducing any possible effects of Pyk2 towards PAG3 in COS-7 cells.

Immunostaning revealed that both endogenous paxillin and PAG3 were widely distributed in the cytoplasm of COS-7 cells, with large regions of overlap (Fig. 19 B). Codistribution of these two proteins at cell periphery was also seen when the focus was adjusted across the center of the nucleus (cell body). Moreover, punctate staining in the cytoplasm was seen with PAG3 and albeit less clearly, with paxillin. Both proteins may be colocalized within some of these punctate structures, but a clear assessment of the colocalization was difficult because of the weak signals and

diffuse distributions of these punctate structures (see later). On the other hand, though PAG3 was still detected near the cell bottom, no significant accumulation of PAG3 was detected at focal adhesion plaques where paxillin was condensed (Fig. 19 B). Therefore, PAG3 is not an integrin-assembly protein at focal adhesions.

Colocalization of PAG3 with ARFs

PAG3 has been shown to exhibit GAP activity in vitro against several ARFs including ARF1, ARF5 and ARF6 (Andreev et al., 1999). We then examined colocalizations between endogenous PAG3 and ARFs, by expressing each HA-ARF isoform cDNA in COS-7 cells.

ARF1 has been shown to be localized at the perinuclear areas, whereas ARF5 and ARF6 were localized throughout the cytoplasm (Peters et al., 1995; Hosaka et al., 1996), as also shown in Fig. 19. Endogenous PAG3 was widely distributed in the cytoplasm in COS-7 cells (see Fig. 19 B), and comparison with different ARF isoforms revealed that PAG3 appeared to overlap with all classes of ARFs; ARF1 (class I), ARF5 (class II) and ARF6 (class III) (Fig. 20). However, colocalization with PAG3 was most readily observed for ARF6 (Fig. 20; g-i). On the other hand, only a fraction of PAG3 was colocalized with ARF1 (Fig. 20; a-c). ARF5 also seeded to be well colocalized with PAG3, but to a lesser extent than ARF6 did (Fig. 20; d-f).

Overexpression of PAG3 does not cause β-COP redistribution

ARF6 has been shown to function primarily at early endosome and plasma membranes but not at pre-Golgi or Golgi, though it shows a wide distribution at cytoplasm including the pre-Golgi structure (Peters et al., 1995). Since PAG3 localization, as in the case of ARF6, also cover the pre-Golgi region where β-COP exists, we examined whether PAG3 could function at the pre-Golgi. To express PAG3 cDNA products at high levels in COS-7 cells, we used pEGFP-C1 vector in which cDNAs were driven by the cytomegalo virus promoter.

It is well known that the inhibition of ARF1 activity by overexpression of its dominant-negative form ARF1 (N126I) can cause the redistribution of β-COP into the cytosol or ER (PETERS ET AL., 1995; OOI ET AL., 1998). This was confirmed with our COS-7 cells (Fig. 21). On the other hand, inhibition of ARF6 has been shown too incapable of causing such redistribution (also see Fig. 21; j-l). We found that the overexpression of PAG3 also did not cause the β-COP redistribution (Fig. 21; m-o). In these PAG3 overexpressing cells, BFA treatment could still cause β-COP redistribution (Fig. 21; p-r).

Possible Functional Interaction between PAG3 and ARFs

We next explored possible functional interaction of PAG3 with ARF activities. Aluminum fluoride (AlF) is a G protein activator that can affect the behavior of ARFs, including ARF1 and ARF6 (Radhkrishna et al., 1996; Ooi et al., 1998). AlF treatment gives rise to distinct cell phenotypes depending on the ARF cDNAs transfected: it increases number and size of ARF1-associated punctate structures in the ARF1-transfected cells (Ooi et al., 1998), and induces membrane protrusion in the ARF6-transfected cells (Fig. 22; a-c) (Radhkrishna et al., 1996). Since these phenotypes induced by the AlF treatment are conspicuous and easily recognized, especially with ARF6-transfected cells, we tested in this system whether overexpression of PAG3

could counteract the ARF activities. We made a mutant PAG3 cDNA (CA mutant) in which the critical cysteine residue (zinc finger motif: CxxCx16CxxC: where x is any amino acid) for the GAP activity was mutated into alanine to diminish the activity (AxxC-x16-CxxC) as negative control. To activate GTP-binding proteins, transfected COS-7 cells were treated for 1 h with 30 mM NaF and 50 mM AlCl3 (AlF) at 37 °C as previously described (Radhakrishna et al., 1996; Ooi et al., 1998), before fixation. As shown in Fig. 22, we found that although overexpression of the CA mutant did not suppress the phenotype of membrane protrusion seen in the ARF6-transfected and AlF-treated cells, overexpression of wild type PAG3 could suppress the phenotype. After the AlF treatment, membrane protrusions were seen with more than 90 % of cells expressing both ARF6 and PAG3 CA mutant. On the other hand, such membrane protrusions were not observed with majority of the ARF6-expressing cells (more than 50-60 % of cells) when the wild type PAG3 was overexpressed. It is also interesting to note that the CA mutant was then clearly colocalized with ARF6 at the membrane protrusions of the cell periphery (Fig. 22; g-i). Similar colocalization of endogenous PAG3 with ARF6 at membrane protrusions was also observed in the ARF6-transfected and AlF-treated cells (Fig. 24 B). On the other hand, in ARF1-transfected cells, a number of very small ARF1-containing punctate structures emerged upon AlF-treatment, that could not be suppressed by the overexpression of PAG3 nor its CA mutant (Fig. 23). Moreover, unlike in the case of ARF6, majority of endogenous PAG3 was not colocalized with ARF1 in the ARF1-transfected and AlF-treated cells (Fig. 24 A).

ARF Activities Affect Subcellular Localization of Paxillin

ARF1 has been shown to be involved in the recruitment of paxillin to focal contacts (Norman et al., 1998). Our results shown above, together with results showing that PAG3 may be a GAP for several ARFs (Andreev et al., 1999), then prompted us to examine whether different classes of ARFs could affect the paxillin subcellular localization. We again employed the AlF-treatment.

With this system, changes in the cellular organizations could be observed within a relatively short time (10 - 120 min), thus enabling the clear comparison of exogenous ARF activities. In our system, exogenous expression of any of ARF1, ARF5 and ARF6 per se did not affect significantly the subcellular localization of endogenous paxillin (data not shown). When these cells were treated with AlF, on the other hand, subcellular distribution of paxillin was drastically changed (Fig. 25). Of these, a significant fraction, but not all, of paxillin then colocalized with ARF6 at several membrane protrusions. Paxillin also appeared to colocalize with ARF1 and ARF5 at some of their punctate structures.

Overexpression of PAG3 Causes Loss of Paxillin Recruitment to Focal Contacts

To explore further the cellular function of PAG3, we next examined the effects of PAG3 overexpression on paxillin localization. As shown in Fig. 26, when PAG3 was overexpressed, no significant staining of paxillin was observed at focal adhesions. Overexpression of the CA mutant of PAG3 did not exert such an effect; thus, this effect appeared to be mediated by the GAP activity of PAG3.

Overexpression of PAG3 Decreases Cell Migratory Activity

Cell adhesion and migratory activities are primarily mediated by integrin adhesion to the ECM. Our results described above prompted us to investigate how much PAG3 is involved in these cell activities on ECMs. Cell adhesion activity was measured with cDNA-transfected COS-7 cells by replating the cells on cell culture dishes coated with various ECMs. Cell migration activity was measured using modified Boyden chambers (Klemke et al, 1998) (see Fig. 27).

As shown in Fig. 28 A, a drastic effect was observed when cell migration activity was

measured. The overexpression of PAG3 caused several fold decreases in the cell migratory activity on these ECMs as compared with those overexpressing the CA mutant. On the other hand, as shown in Fig. 28 B, only marginal differences were observed among untransfected cells and cells overexpressing PAG3 and the CA mutant with regard to the cell adhesion activity on collagen, fibronectin and vitronectin. Rate of the cell spreading was also not affected significantly by the overexpression of PAG3 or the CA mutant as compared to the untransfected cells (data not shown). cDNA transfection efficiencies measured by counting the transfection-positive cells identified by the fluorescence from the EGFP tag, and levels of exogenous protein expression measured by immunoblotting analysis were essentially the same between PAG3 and the CA mutant. These data provide quantitative evidence further supporting our analysis.

Finally, we also examined exogenous expression of EGFP-PAG3 with U937 monocyte cells differentiated by TPA. Again, overexpression of EGFP-PAG3 seemed to act to decrease the heptotactic activity as compared to expression of the CA mutant or the mock-transfection, while the cell adhesion activity was almost unaffected (Fig. 28).

DISCUSSION

Integrins play essential roles in a number of dynamic aspects of cell regulation including migration and trans-invasion. Integrin function requires assembly of a number of different proteins at the integrin cytoplasmic domains. Therefore, it is believed that mechanisms that orchestrate protein assembly at the cytoplasmic tails of integrins might exist, and considerable effort has been devoted to identification of such mechanisms (reviewed in Burridge and Chrzanowska-Wodnicka, 1996). We have shown previously in fibroblasts that cytoplasmic protein paxillin, which functions as an integrin adapter, appears to localize to the perinuclear area of the cell (Mazaki et al., 1998). In this paper, we isolated a new paxillin-binding protein PAG3 and provided evidence that cellular ARF activities are involved in the subcellular localization and the focal contact recruitment of paxillin, as well as in the regulation of cell migratory activities.

We identified PAG3 from mature monocyte cells, and showed that PAG3 expression is highly induced during monocyte maturation, accompanied by its tyrosine phosphorylation. Upon monocyte maturation, integrins are activated and cells become adherent, motile and trans-invasive into tissues. We have shown that expression of all the three isoforms of paxillin also increased upon monocyte maturation and become highly phosphorylated (Mazaki et al., 1997). Our results in this paper revealed that both PAG3 and paxillin are recruited to the cell periphery in mature monocytes adhered to the ECM. We also demonstrated that PAG3 binding to paxillin is increased during monocyte maturation while the binding to Pyk2 is almost unchanged. Moreover, we demonstrated that PAG3 overexpression could inhibit paxillin recruitment to focal adhesions and cell migratory activity. Thus, PAG3 seems to play an important role in the integrin activation and function that are taken place during monocyte maturation. Andreev et al. has also suggested that PAG3 can be tyrosine phosphorylated by Pyk2 and by Src family kinases (Andreev et al. 1999). These kinases exist in monocyte cells, and it would be also interesting to analyze the physiological role of tyrosine phosphorylation of PAG3 in monocyte cells. However, due to their small

cytoplasm, haematopoietic cells including monocytes in general are not suitable for the analysis of intracellular protein localization or organelle structure. A relatively low efficiency of DNA transfection also hampers precise analysis. Thus, we have not yet described the precise mechanism of PAG3 function in monocyte cells.

PAG3 is identical to the recently described proteins PAPα (Andreev et al., 1999). PAPα has been identified as a Pyk2-binding protein, and was shown to exhibit strong in vitro GAP activity towards ARF1 and ARF5, but 102- to 103-fold less activity towards ARF6. ARF1 colocalizes with β-COP and regulate its subcellular localization. The subcellular localization of endogenous PAG3 includes β-COP-containing structures, as previously shown (Andreev et al., 1999), although PAG3 exhibited a much broader distribution in the cytoplasm. The subcellular localization of ARF6 also includes the pre-Golgi structure, but inhibition of ARF6 activity does not affect the cellular distribution of β-COP (Peters et al., 1995). Likewise, our results and those of others (Andreev et al., 1999) showed that PAG3 does not affect the subcellular localization of β-COP, while we confirmed that inhibition of ARF1 does affect it in our cell culture (data not shown), as shown previously (Peters et al., 1995). We also showed that PAG3 is clearly colocalized with ARF6 in the AlF-treated ARF6-transfected cells. Moreover, we demonstrated that PAG3, but not its GAP-inactive mutant, can be inhibitory of the AlF-induction of ARF6 activity in vivo. Taken together, our results suggest that ARF6 is an in vivo target of the GAP activity of PAG3, even though a previous study demonstrated that PAG3 exhibits only a weak activity towards ARF6 in vitro (Andreev et al., 1999). In this regard, it has been reported that coatomer protein directly participates in the GTPase reaction of ARF1GAP, accelerating GTP hydrolysis by ARF1 an additional 1000-fold (Goldberg, 1999). The previous study by Andreev et al., however, was done without the addition of a coatomer protein. Our analysis implies that PAG3 function involves ARF6, and it remains to be determined how efficiently PAG3 can interact with ARF1 in vivo.

The function of ARF5, a class II ARF isoform, has not been well studied. Therefore, we did not assess the interaction between ARF5 and PAG3 in detail. Our preliminary data indicate that the subcellular distributions of ARF5 and PAG3 overlap but there is one significant difference:

an ARF5 dominant-negative mutant caused redistribution of β-COP, whereas PAG3 did not. However, different GAP proteins may be involved in the recruitment of different coatomer proteins to the same ARF (Springer et al., 1999). Thus, like in the case of the relationship of PAG3 with ARF1 as described above, our results do not preclude interaction of the PAG3 with ARF5 in vivo.

We showed that all the three classes of ARF activities could influence the subcellular localization of paxillin. Among the ARFs, colocalization with PAG3 is readily observed for ARF6, especially in the ARF6-transfected and AlF-treated cells. ARF6 primarily functions at or near the cell periphery. Our previous analysis in fibroblast cells, however, indicates that a major fraction of cytoplasmic paxillin in fibroblasts is localized at a perinuclear region which largely overlaps with the Golgi marker Golgi 58K protein (Mazaki et al., 1998) and the pre-Golgi coatomer protein β-COP (unpublished data). On the other hand, cells such as epithelial cells exhibit a relatively diffuse distribution of paxillin in the cytoplasm (see Fig. 19 B). We have identified several paxillin-binding proteins bearing ARFGAP activities (PAGs), and found that one of them, PAG1, is active primarily toward ARF1 (to be published elsewhere). We have also obtained a result showing that both ARF1 and PAG1 activities are involved in the regulation of the perinuclear localization of paxillin and β-COP. Therefore, PAG3 is not the sole protein that binds to and regulates the subcellular localization of paxillin. Similarly, ARF6 is not the only ARF protein that regulates the subcellular localization of paxillin, since ARF1 may also play this role, as previously described (Norman et al., 1998).

PAG3 has multiple protein-protein interaction domains. Our preliminary experiment suggests that several yet unidentified proteins interact with PAG3, in addition to paxillin, Pyk2 and ARF6. We showed that PAG3 overexpression acts inhibitory for the cell migratory activity. We thus tested whether the co-overexpression of dominant-active form of ARF6 (ARF6Q67L) could restore the migratory activity, and found that this was not the case our unpublished results). This result is also consistent with the above notion that PAG3 may not only act on ARF6 to cause the retardation in the cell migratory activity.

PAG3 also contains a lipid interacting PH domain. Andreev et al. have shown that PAG3 indeed requires the addition of phosphatidyl-4, 5,bis-phosphates (PIP2) for its ARFGAP activity in vitro. Several other ARFGAP proteins, such as ASAP (Brown et al., 1998), also contain the PH domain. PIP2 has also been shown to stimulate the ARFGAP activity of ASAP, through its binding to the PH domain (Brown et al., 1998).

Their PH domains, however, appear to bind to PIP3 more strongly than to PIP2. In contrast, PIP3 seems to be ineffective on the ARFGAP activity of ASAP (Brown et al.1998). Thus, it is possible that regulating PIP2 and PIP3 levels by lipid metabolism, in which ARF and Rho have been implicated, may, in turn, regulate the ARF activities. Thus, there seems to exist a feedback loop of the regulation of ARF activities through the regulation of lipid metabolites.

Hypothetical Model

Our current study cannot determine whether or not PAG3 is involved in the dynamic process of the hypothesized intracellular transport of paxillin. We also do not know how the activity of PAG3 relates to the regulation of actin stress fiber formation. Furthermore, we also do not know to what extent the inhibition of paxillin recruitment to focal contacts caused by the overexpression of PAG3 relates to the inhibition of cell migratory activities.

ARF-family proteins are implicated in the regulation of membrane and vesicle traffic in mammalian cells. However, recent studies suggests that the function of ARF proteins also involves regulation of actin cytoskeletal organization (Peter et al., 1995; Norman et al., 1998; Radhakrishna et al., 1999) (see Fig. 29). Norman et al., showed that ARF1 participates in the regulation of the focal adhesion recruitment of paxillin and also in the regulation of Rho-stimulated stress fiber formation; thus implicating the intercommunication of these two different families of small GTP binding proteins.

How are the membrane trafficking processes regulated by ARF activity related to the subcellular localization of paxillin, as well as cell adhesive and migratory activity? Previous studies have shown that ARF6 is localized at the cell periphery, and cycles between the plasma membrane and intracellular endosomal vesicles, depending on its nucleotide status (D'Souza-Schorey et al, 1995; Peters et al., 1995). Paxillin and PAG3 are colocalized at several areas within a cell, whereas PAG3 is not observed in focal contacts of adhesion plaques. We showed that overexpression of PAG3, but not its GAP-mutant, inhibits paxillin recruitment to focal adhesion plaques. These results are consistent with the hypothesis that PAG3 may be involved in the intracellular transport of paxillin, but is not one of the components of integrin-assembly proteins at the focal adhesions. Punctate staining of PAG3 in the cytoplasm suggests that PAG3 may associate with cytoplasmic vesicles. Since membrane traffic is primarily involved in the intracellular transport of membrane or secretory proteins, one simple explanation could be that cytoplasmic paxillin is already associated with a membrane protein inserted in transport vesicles. This membrane protein may be an integrin, as also suggested previously (Norman et al., 1998) (see Fig. 30). However, Miyamoto et al. have suggested that paxillin is recruited to the cytoplasmic regions of integrins only after the cell surface integrins are cross-linked, and thus seems to be non-essential for the translocation of integrins to the plasma membrane (Miyamoto et al., 1995). Alternatively, since PAG3 appears to associate directly with membranes through its PH domain (Andreev et al., 1999), binding of paxillin with PAG3 may enable an association and/or interaction of paxillin with the vesicle membrane, and may be thus involved in its putative intracellular transport along membrane trafficking pathways. Consistent with this, recent model suggests that ARFGAP proteins localize constantly on the budding vesicles (Springer et al., 1999) (see Fig. 31).

Alternatively, apart from the vesicle transport activity, ARF activities may be more directly involved in the regulation of actin cytoskeletal organization as well as paxillin-containing focal adhesion formation, in which Rho-family GTPases have been implicated to play crucial roles (see Fig. 29 and 30). D'Souza-Schorey et al. (1997) has been reported that ARF6 is also involved in

cytoskeletal remodeling, possibly through its direct interaction with a Rac-interacting protein, Partner of Rac1 (POR1). This also suggest the intercommunication between ARF6 and Rac1, which regulates actin cytoskeletal organization; and implicates that ARF6 thus contributes to establish highly specified regulation of cytoskeletal reorganization as well as the plasma membrane architecture. Conversely, a member of the Rho family RhoD, for example, has been demonstrated to provide a molecular link between intracellular transport and actin cytoskeleton (Murphy et al., 1996). A number of recent studies have begun to unveil the interdependence and cross-talk among otherwise unrelated signaling pathways that ultimately determine the overall cytoskeletal as well as organelle organization (see Fig. 32).

In conclusion, our present study, together with the previous study of Norman et al. (1998), revealed that the intracellular dynamics of paxillin and its focal adhesion recruitment are not mediated by a free cytoplasmic diffusion, but are under the control of activities of ARF-family GTP-binding proteins and ARFGAP proteins. The binding of paxillin towards the ARFGAP protein implies that focal adhesion recruitment of paxillin may simultaneously regulate this intracellular process. Further analysis to determine the precise mechanism of PAG3 function will provide further insight not only into the regulation of paxillin subcellular localization, but also into the regulation of cell migratory activity through the regulation of ARF activities.

ACKNOWLEDGMENTS

I am deeply grateful to Hisataka Sabe for his direction and discussion throughout this study. I am indebted to Shigeru Hashimoto, Yuichi Mazaki and Hajime Yano for their contributions to this study and their valuable discussions; and Juan Bonifacino, Victor Hsu and Yasuhiro Minami for their valuable discussions and comments. I thank to Mihoko Sato and Manami Hiraishi for their technical assistants, also thank to K. Nakayama for his generous gift of ARF cDNAs and useful discussions, T. Nagase for KIAA0400 cDNA and T. Sasaki for Pyk2 antibody. I finally thank to Kuniaki Nagayama for his warm-hearted Mentorship for me.

REFERENCES

Andreev, J., Simon, J. P., Sabatini, D. D., Kam, J., Plowman, G., Randazzo, P. A., and Schlessinger, J. (1999). Identification of a new Pyk2 target protein with Arf-GAP activity. Mol. Cell. Biol. 19, 2338-2350.

Balch, W. E., Kahn, R. A., and Schwaninger, R. (1992). ADP-ribosylation factor is required for vesicular trafficking between the endoplasmic reticulum and the cis-Golgi compartment. J. Biol. Chem. 267, 13053-13061.

Boman, A. L., and Kahn, R. A. (1995). Arf proteins: the membrane traffic police? Trends Biochem. Sci. 20, 147-150.

Bonifacino, J. S., Suzuki, C. K., Lippincott-Schwartz, J., Weissman, A. M., and Klausner, R. D. (1989). Pre-Golgi degradation of newly synthesized T-cell antigen receptor chains: intrinsic sensitivity and the role of subunit assembly. J. Cell Biol. 109, 73-83.

Brown, H. A., Gutowski, S., Moomaw, C. R., Slaughter, C., and Sternweis, P. C. (1993). ADP-ribosylation factor, a small GTP-dependent regulatory protein, stimulates phospholipase D activity. Cell 75, 1137-1144.

Brown, M. T., Andrade, J., Radhakrishna, H., Donaldson, J. G., Cooper, J. A., and Randazzo, P. A. (1998). ASAP1, a phospholipid-dependent arf GTPase-activating protein that associates with and is phosphorylated by Src. Mol. Cell. Biol. 18, 7038-7051.

Burridge, K., and Chrzanowska-Wodnicka, M. (1996). Focal adhesions, contractility, and signaling.

Annu. Rev. Cell Dev. Biol. 12, 463-518.

Burridge, K., Turner, C. E., and Romer, L. H. (1992). Tyrosine phosphorylation of paxillin and pp125FAK accompanies cell adhesion to extracellular matrix: a role in cytoskeletal assembly. J. Cell Biol. 119, 893-903.

Clark, E. A., and Brugge, J. S. (1995). Integrins and signal transduction pathways: the road taken. Science 268, 233-239.

Clark, J., Moore, L., Krasinskas, A., Way, J., Battey, J., Tamkun, J., and Kahn, R. A. (1993). Selective amplification of additional members of the ADP-ribosylation factor (ARF) family: cloning of additional human and Drosophila ARF-like genes. Proc. Natl. Acad. Sci. USA 90, 8952-8956.

Cockcroft, S. (1996). ARF-regulated phospholipase D: a potential role in membrane traffic. Chem. Phys. Lipids 80, 59-80.

Cukierman, E., Huber, I., Rotman, M., and Cassel, D. (1995). The ARF1 GTPase-activating protein: zinc finger motif and Golgi complex localization. Science 270, 1999-2002.

D'Souza-Schorey, C., Guangpu, L., Colombo, M. I., and Stahl, P. D. (1995). A regulatory role for ARF6 in receptor-mediated endocytosis. Science 267, 1175-1178.

Dascher, C., and Balch, W. E. (1994). Dominant inhibitory mutants of ARF1 block endoplasmic reticulum to Golgi transport and trigger disassembly of the Golgi apparatus. J. Biol. Chem. 269, 1437-1448.

Dell'Angelica, C. E., Mullins, C., Bonifacino, S. J. (1999). AP-4, a Novel Protein Complex Related to Clathrin Adaptors. J. Biol. Chem. 274, 7278-7285.

Dittie, A. S., SHajibagheri, N., and Tooze, S. A. (1996). The AP-1 adaptor complex binds to immature secretory granules from PC12 cells, and is regulated by ADP-ribosylation factor. J. Cell Biol. 132, 523-536.

Donaldson, J. G., Cassel, D., Kahn, R. A., and Klausner, R. D. (1992). ADP-ribosylation factor, a small GTP-binding protein, is required for binding of the coatomer protein beta-COP to Golgi membranes. Proc. Natl. Acad. Sci. USA 89, 6408-6412.

Donaldson, J. G., and Klausner, R. D. (1994). ARF: a key regulatory switch in membrane traffic and organelle structure. Curr. Opin. Cell Biol. 6, 527-532.

Gidlund, M., Orn, A., Pattengale, P. K., Jansson, M., Wigzell, H., and Nilsson, K. (1981). Natural killer cells kill tumour cells at a given stage of differentiation. Nature 292, 848-850.

Goldberg, J. (1999). Structural and functional analysis of the ARF1-ARFGAP complex reveals a role for coatomer in GTP hydrolysis. Cell 96, 893-902.

Graham, I. L., Anderson, D. C., Holers, V. M., and Brown, E. J. (1994). Complement receptor 3 (CR3, Mac-1, integrin alpha M beta 2, CD11b/CD18) is required for tyrosine phosphorylation of paxillin in adherent and nonadherent neutrophils. J. Cell Biol. 127, 1139-1147.

Ha, K. S., Yeo, E. J., and Exton, J. H. (1994). Lysophosphatidic acid activation of

phosphatidylcholine-hydrolysing phospholipase D and actin polymerization by a pertussis toxin-sensitive mechanism. Biochem. J. 303, 55-59.

Hall, A. (1994). Small GTP-binding proteins and the regulation of the actin cytoskeleton. Annu. Rev. Cell Biol. 10, 31-54.

Hall, A. (1998). Rho GTPases and the actin cytoskeleton. Science 279, 509-514.

Hynes, R. O. (1992). Specificity of cell adhesion in development: the cadherin superfamily. Curr. Opin. Genet. Dev. 2, 621-614.

Ishikawa, K., Nagase, T., Nakajima, D., Seki, N., Ohira, M., Miyajima, N., Tanaka, A., Kotani, H., Nomura, N., and Ohara, O. (1997). Prediction of the coding sequences of unidentified human genes. VIII. 78 new cDNA clones from brain which code for large proteins in vitro. DNA Res. 4, 307-313.

Kaelin Jr., W. G., Krek, W., Sellers, W. R., DeCaprio, J. A., Ajchenbaum, F., FuchsCS, C. S., ChittendenT, T., Li, Y., FarnhamPJ, P. J., Blanar, M. A., Livingston, D. M., and Flemington, E. K. (1992). Expression cloning of a cDNA encoding a retinoblastoma-binding protein with E2F-like properties. Cell 70, 351-364.

Kahn, R. A., and Gilman, A. G. (1986). The protein cofactor necessary for ADP-ribosylation of Gs by cholera toxin is itself a GTP binding protein. J. Biol. Chem. 261, 7906-7911.

Kahn, R. A., Randazzo, P., Serafini, T., Weiss, O., Rulka, C., Clark, J., Amherdt, M., Roller, P., Orci, L., and Rothman, J. E. (1992). The amino terminus of ADP-ribosylation factor (ARF) is a critical determinant of ARF activities and is a potent and specific inhibitor of protein transport. J.

Biol. Chem. 267, 13039-13046.

Kahn, R. A., Yucel, J. K., and Malhotra, V. (1993). ARF signaling: a potential role for phospholipase D in membrane traffic. Cell 75, 1045-1048.

Klemke, R. L., Leng, J., Molander, R., Brooks, P. C., Vuori, K., and Cheresh, D. A. (1998). CAS/Crk coupling serves as a "molecular switch" for induction of cell migration. J. Cell Biol. 140, 961-972.

Lauffenburger, D. A., and Horwitz, A. F. (1996). Cell migration: a physically integrated molecular process. Cell 84, 359-369.

Lenhard, J. M., Kahn, R. A., and Stahl, P. D. (1992). Evidence for ADP-ribosylation factor (ARF) as a regulator of in vitro endosome-endosome fusion. J. Biol. Chem. 267, 13047-13052.

Mayer, B. J., Hirai, H., and Sakai, R. (1995). Evidence that SH2 domains promote processive phosphorylation by protein-tyrosine kinases. Curr. Biol. 5, 296-305.

Mazaki, Y., Hashimoto, S., and Sabe, H. (1997). Monocyte cells and cancer cells express novel paxillin isoforms with different binding properties to focal adhesion proteins. J. Biol. Chem. 272, 7437-7444.

Mazaki, Y., Uchida, H., Hino, O., Hashimoto, S., and Sabe, H. (1998). Paxillin isoforms in mouse. Lack of the gamma isoform and developmentally specific beta isoform expression. J. Biol. Chem. 273, 22435-22441.

Miyamoto, S., Teramoto, H., Coso, O. A., Gutkind, J. S., Burbelo, p. D., Akiyama, S. K., and

Yamada, K. M. (1995). Integrin function: molecular hierarchies of cytoskeletal and signaling molecules. J. Cell Biol. 131, 791-805.

Norman, J. C., Jones, D., Barry, S. T., Holt, M. R., Cockcroft, S., and Critchley, D. R. (1998). ARF1 mediates paxillin recruitment to focal adhesions and potentiates Rho-stimulated stress fiber formation in intact and permeabilized Swiss 3T3 fibroblasts. J. Cell Biol. 143, 1981-1995.

Nuoffer, C., and Balch, W. E. (1994). GTPases: multifunctional molecular switches regulating vesicular traffic. Annu. Rev. Biochem. 63, 949-990.

Ooi, C. E., Dell'Angelica, E. C., and Bonifacino, J. S. (1998). ADP-Ribosylation factor 1 (ARF1) regulates recruitment of the AP-3 adaptor complex to membranes. J. Cell Biol. 142, 391-402.

Peters, P. J., Hsu, V. W., Ooi, C. E., Finazzi, D., B.Teal, S., Oorschot, V., Donaldson, J. G., and Klausner, R. D. (1995). Overexpression of wild-type and mutant ARF1 and ARF6: distinct perturbations of nonoverlapping membrane compartments. J. Cell Biol. 128, 1003-1017.

Poon, P. P., Wang, X., Rotman, M., Huber, I., Cukierman, E., Cassel, D., Singer, R. A., and Johnston, G. C. (1996). Saccharomyces cerevisiae Gcs1 is an ADP-ribosylation factor GTPase-activating protein. Proc. Natl. Acad. Sci. USA 93, 10074-10077.

Radhakrishna, H., Al-Awar, O., Khachikian, Z., and Donaldson, J. G. (1999). ARF6 requirement for Rac ruffling suggests a role for membrane trafficking in cortical actin rearrangements. J. Cell Sci. 112, 855-866.

Radhakrishna, H., and Donaldson, J. G. (1997). ADP-ribosylation factor 6 regulates a novel plasma membrane recycling pathway. J. Cell Biol. 139, 49-61.

Radhakrishna, H., Klausner, R. D., and Donaldson, J. G. (1996). Aluminum fluoride stimulates surface protrusions in cells overexpressing the ARF6 GTPase. J. Cell Biol. 134, 935-947.

Regen, C. M., and Horwitz, A. F. (1992). Dynamics of beta 1 integrin-mediated adhesive contacts in motile fibroblasts. J. Cell Biol. 119, 1347-1359.

Ridley, A. J., and Hall, A. (1992). The small GTP-binding protein rho regulates the assembly of focal adhesions and actin stress fibers in response to growth factors. Cell 70, 389-399.

Sabe, H., Hata, A., Okada, M., Nakagawa, H., and Hanafusa, H. (1994). Analysis of the binding of the Src homology 2 domain of Csk to tyrosine-phosphorylated proteins in the suppression and mitotic activation of c-Src. Proc. Natl. Acad. Sci. USA 91, 3984-3988.

Sambrook, J., Fritsch, E. F., and Maniatis, T. (1989). In: Molecular Cloning: a laboratory manual, Cold Spring Harbor, NY: Cold Spring Harbor Laboratory Press.

Schekman, R., and Orci, L. (1996). Coat proteins and vesicle budding. Science 271, 1526-1533.

Serafini, T., Orci, L., Amherdt, M., Brunner, M., Kahn, R. A., and Rothman, J. E. (1991). ADP-ribosylation factor is a subunit of the coat of Golgi-derived COP-coated vesicles: a novel role for a GTP-binding protein. Cell 67, 239-253.

Sheetz, M. P., Felsenfeld, D. P., and Galbraith, C. G. (1998). Cell migration: regulation of force on extracellular-matrix-integrin complexes. Trends Cell Biol. 8, 51-54.

Siddiqui, R. A., and English, D. (1997). Phosphatidic acid elicits calcium mobilization and actin polymerization through a tyrosine kinase-dependent process in human neutrophils: a mechanism for induction of chemotaxis. Biochim. Biophys. Acta. 1349, 81-95.

Song, J., Khachikian, Z., Radhakrishna, H., and Donaldson, J. G. (1998). Localization of endogenous ARF6 to sites of cortical actin rearrangement and involvement of ARF6 in cell spreading. J. Cell Sci. 111, 2257-2267.

Springer, S., Spang, A., and Schekman, R. (1999). A primer on vesicle budding. Cell. 97, 145-148.

Stamnes, M.A., and Rothman, J. E. (1993). The binding of AP-1 clathrin adaptor particles to Golgi membranes requires ADP-ribosylation factor, a small GTP-binding protein. Cell 73, 999-1005.

Stearns, T., Willingham, M. C., Botstein, D., and Kahn, R. A. (1990). ADP-ribosylation factor is functionally and physically associated with the Golgi complex. Proc. Natl. Acad. Sci. USA 87, 1238-1242.

Taylor, T. C., Kahn, R. A., and Melancon, P. (1992). Two distinct members of the ADP-ribosylation factor family of GTP-binding proteins regulate cell-free intra-Golgi transport. Cell 70, 69-79.

Tong, X., and Howley, P. M. (1997). The bovine papillomavirus E6 oncoprotein interacts with paxillin and disrupts the actin cytoskeleton. Proc. Natl. Acad. Sci. USA 94, 4412-4417.

Tong, X., Salgia, R., Li, J.-L., Griffin, J. D., and Howley, P. M. (1997). The bovine papillomavirus E6 protein binds to the LD motif repeats of paxillin and blocks its interaction with vinculin and the focal adhesion kinase. J. Biol. Chem. 272, 33373-33376.

Tsuchiya, M., Price, S. R., Tsai, S.-C., Moss, J., and Vaughan, M. (1991). Molecular identification of ADP-ribosylation factor mRNAs and their expression in mammalian cells. J. Biol. Chem. 266, 2772-2777.

Turner, C. E. (1998). Paxillin. Int. J. Biochem. Cell Biol. 30, 955-959.

Turner, C. E., Brown, M. C., Perrotta, J. A., Riedy, M. C., Nikolopoulos, S. N., McDonald, A. R., Bagrodia, S., Thomas, S., and Leventhal, P. S. (1999). Paxillin LD4 motif binds PAK and PIX through a novel 95-kD ankyrin repeat, ARF-GAP protein: a role in cytoskeletal remodeling. J. Cell Biol. 145, 851-863.

West, M. A., Bright, N. A., and Robinson, M. S. (1997). The role of ADP-ribosylation factor and phospholipase D in adaptor recruitment. J. Cell Biol. 138, 1239-1254.

Yamabhai, M., and Kay, B. K. (1997). Examining the specificity of Src homology 3 domain--ligand interactions with alkaline phosphatase fusion proteins. Anal. Biochem. 247, 143-151.

Zhang, C.-j., Rosenwald, A. G., Willingham, M. C., Skuntz, S., Clark, J., and Kahn, R. A. (1994). Expression of a dominant allele of human ARF1 inhibits membrane traffic in vivo. J. Cell Biol. 124, 289-300.

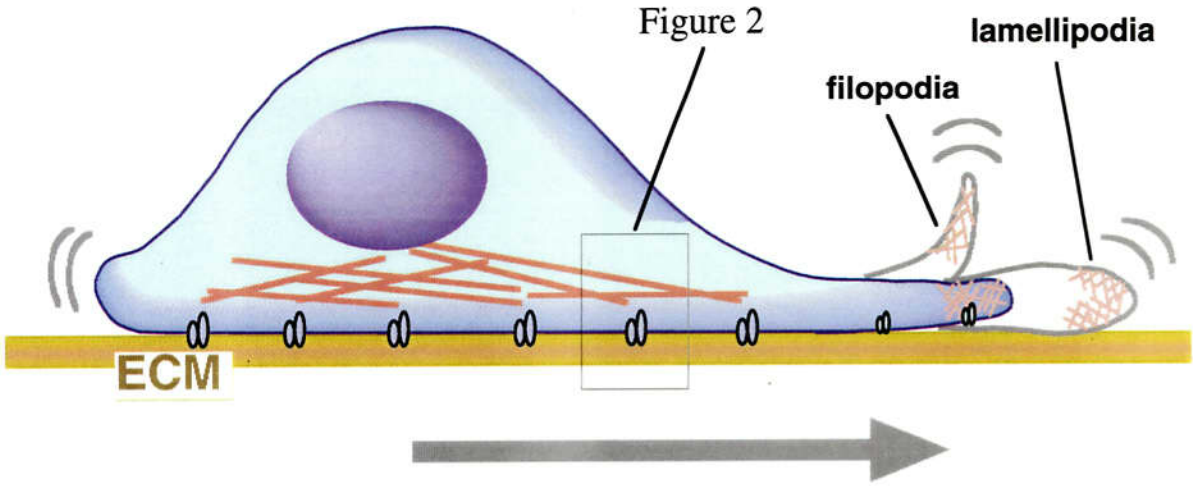

actin mesh

actin stress fiber

focal adhesion

focal complex (small nascent adhesive complex)

Figure 1 Moving Cell

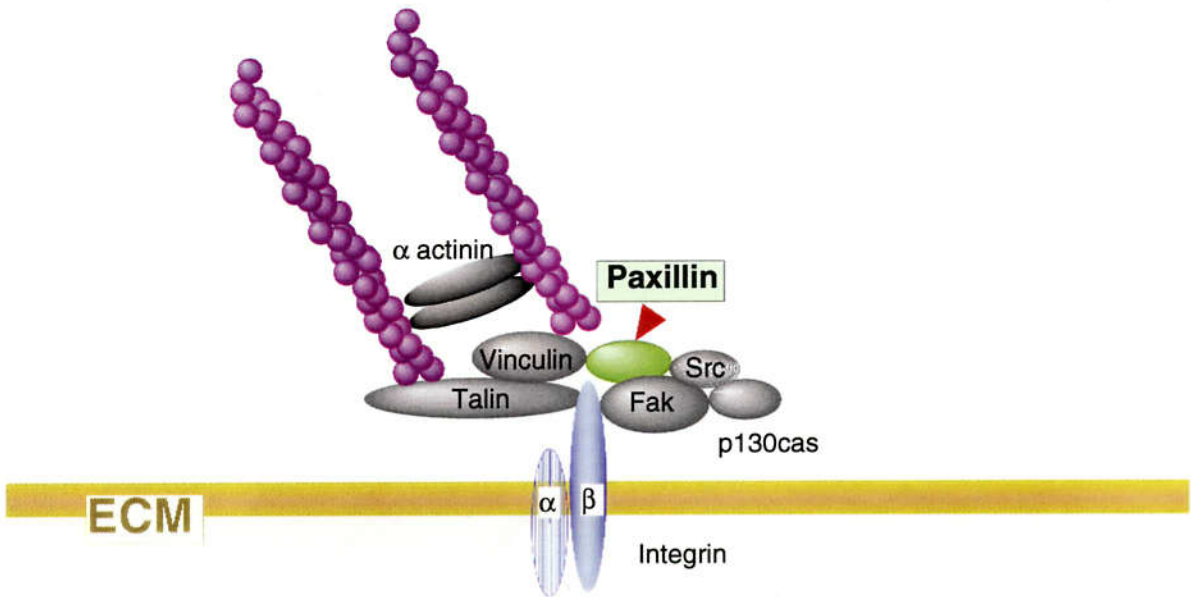

Figure 2 Focal Adhesion

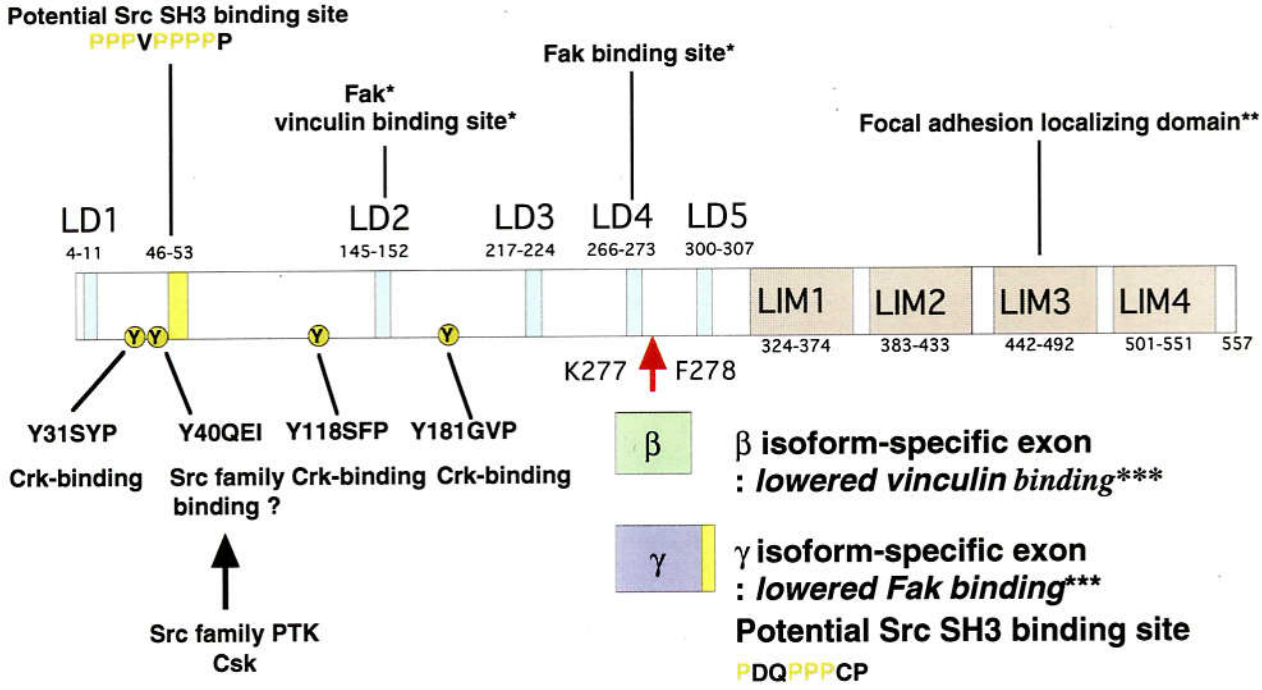

Figure 3 Structure of Human Paxillin
GenBank Ac. : U14588
*(LD motifs) ; Brown MC et al., *Nature Struct. Biol.* 5 : 677-678, 1998
** ; Brown MC et al., *JCB.* 135(4) : 1109-1123, 1996
*** ; Mazaki Y et al., *JBC.* 272(11) : 7437-7444, 1997

Structure of PAG3

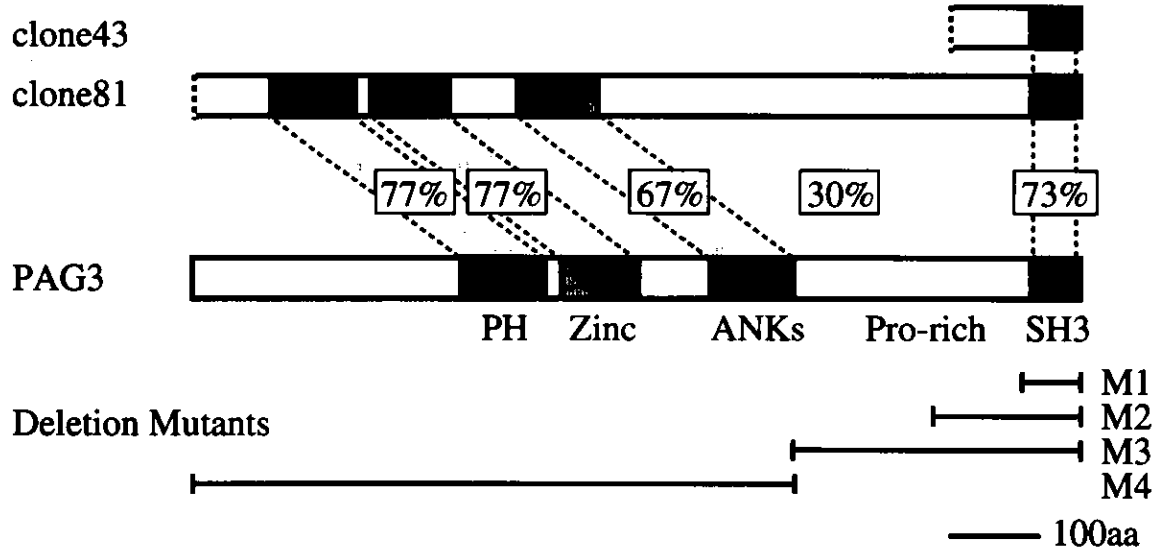

Figure 4 Schematic diagram of PAG3 and its comparison with original two clones isolated using GST-paxillin a as a probe (clone 43 and 81). aa, amino acid.

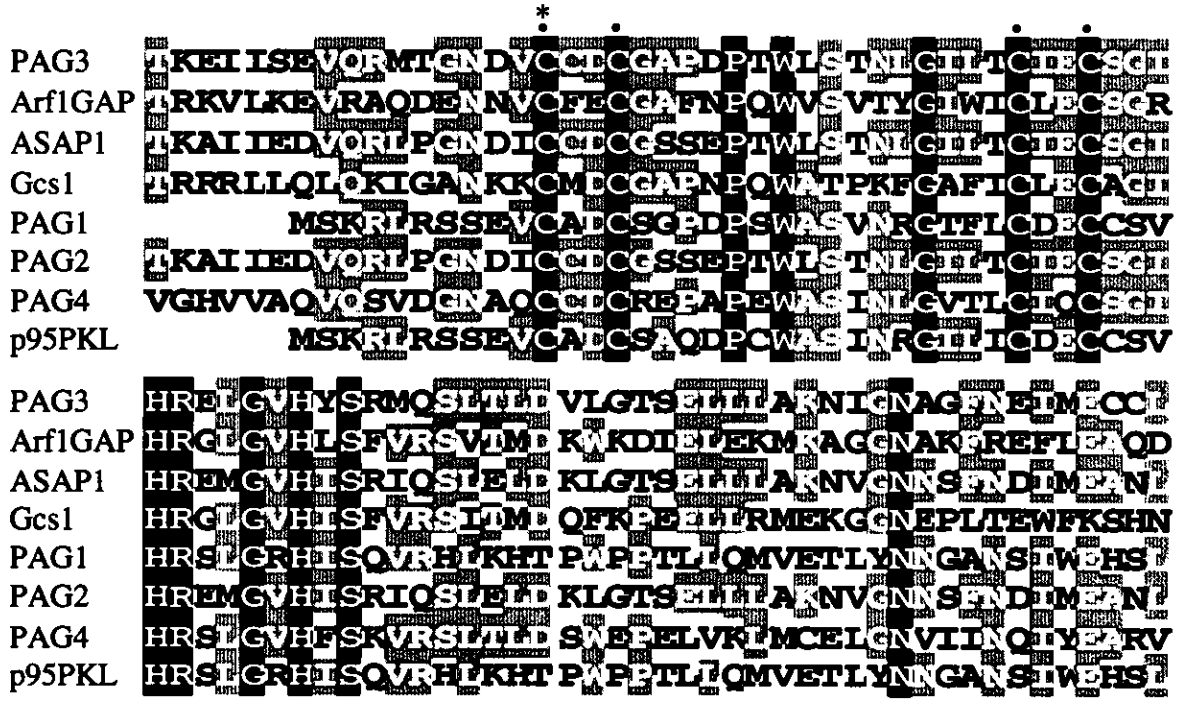

Figure 5 Comparison of the zinc finger domain of PAG3 (residues 420 to 505) with those of ARF1 GAP (residues 6 to 91), ASAP1 (residues 453 to 538; Brown et al., 1998), GCS1 (residues 10 to 95), PAG1 (residues 1 to 83), PAG2 (which corresponds to clone 81), PAG4 (residues 404 to 489) and p95PKL (residues 1 to 83). The cDNA for PAG2 was not complete, therefore, residue numbers were not assigned. Identical residues are framed and shadowed. The positions of four conserved cysteines of the zinc finger motif are marked by dots, and the residue mutated in the PAG3 CA mutant is marked by an asterisk. ASAP1 corresponds to the s19 clone, and PAG1, PAG2 and PAG4 correspond to our collection of paxillin-binding proteins (unpublished).

```
      10        20        30        40        50        60        70        80        90
atgccggaccagatctccgtgtcggaattcgtggccgagacccatgaggactacaaggcgcccacggcctccagcttcaccacccgcacg
M  P  D  Q  I  S  V  S  E  F  V  A  E  T  H  E  D  Y  K  A  P  T  A  S  S  F  T  T  R  T

     100       110       120       130       140       150       160       170       180
gcgcagtgccggaacactgtggcggccatcgaggaggctttggacgtggaccggatggttctttacaaaatgaagaaatccgtgaaagca
A  Q  C  R  N  T  V  A  A  I  E  E  A  L  D  V  D  R  M  V  L  Y  K  M  K  K  S  V  K  A

     190       200       210       220       230       240       250       260       270
atcaacagctctgggctggctcacgtggaaaatgaagagcagtacacccaggctctggagaagtttggcggcaactgtgtatgcagagat
I  N  S  S  G  L  A  H  V  E  N  E  E  Q  Y  T  Q  A  L  E  K  F  G  G  N  C  V  C  R  D

       280       290       300       310       320       330       340       350       360
gacccagatttaggaagtgcgttcctgaagttctcagtgtttacaaaggagttgacagcacttttcaaaaacctgattcagaatatgaac
D  P  D  L  G  S  A  F  L  K  F  S  V  F  T  K  E  L  T  A  L  F  K  N  L  I  Q  N  M  N

     370       380       390       400       410       420       430       440       450
aacataatctccttccctttggacagtttgctgaaggggacctgaaaggagtgaaaggggatctgaaaaagccttttgataaagcttgg
N  I  I  S  F  P  L  D  S  L  L  K  G  D  L  K  G  V  K  G  D  L  K  K  P  F  D  K  A  W

     460       470       480       490       500       510       520       530       540
aaggactatgaaacaaaaataaccaagatagaaaaggagaaaaaggaacacgccaagctccatgggatgattcggactgaaataagcgga
K  D  Y  E  T  K  I  T  K  I  E  K  E  K  K  E  H  A  K  L  H  G  M  I  R  T  E  I  S  G

     550       560       570       580       590       600       610       620       630
gcggaaattgccgaagagatggaaaaggagaggcgcttcttccagctacagatgtgcgagtatctgctgaaggtcaacgaaatcaagatt
A  E  I  A  E  E  M  E  K  E  R  R  F  F  Q  L  Q  M  C  E  Y  L  L  K  V  N  E  I  K  I

     640       650       660       670       680       690       700       710       720
aaaaagggagtagatttacttcagaatctgatcaaatactttcatgcccaatgcaatttttttcaggatggactcaaagccgtggaaagc
K  K  G  V  D  L  L  Q  N  L  I  K  Y  F  H  A  Q  C  N  F  F  Q  D  G  L  K  A  V  E  S

     730       740       750       760       770       780       790       800       810
ctcaaaccttccattgaaacgctgtctacggatcttcacacgatcaaacaggcccaggatgaagaaagaaggcagttgatacagcttcga
L  K  P  S  I  E  T  L  S  T  D  L  H  T  I  K  Q  A  Q  D  E  E  R  R  Q  L  I  Q  L  R

     820       830       840       850       860       870       880       890       900
gatattttgaaatccgcattgcaggttgaacagaaagaggactcccaaattcgtcagagcacagcttatagcttacatcagcctcaggga
D  I  L  K  S  A  L  Q  V  E  Q  K  E  D  S  Q  I  R  Q  S  T  A  Y  S  L  H  Q  P  Q  G

     910       920       930       940       950       960       970       980       990
aacaaggaacatgggaccgagcggaacggcagcctctacaagaagagtgacgggatccgaaaagtgtggcagaaaaggaaatgttcagtt
N  K  E  H  G  T  E  R  N  G  S  L  Y  K  K  S  D  G  I  R  K  V  W  Q  K  R  K  C  S  V

    1000      1010      1020      1030      1040      1050      1060      1070      1080
aaaaatggttttctgaccatatcccatggtaccgctaaccggcctcctgcaaagctcaacctgctaacctgccaggtgaagaccaaccct
K  N  G  F  L  T  I  S  H  G  T  A  N  R  P  P  A  K  L  N  L  L  T  C  Q  V  K  T  N  P
```

PH

1090 1100 1110 1120 1130 1140 1150 1160 1170

gaggagaagaagtgctttgaccttatttcacatgacagaacttaccactttcaagctgaagatgaacaggaatgtcaaatatggatgtct

E E K K C F D L I S H D R T Y H F Q A E D E Q E C Q I W M S

1180 1190 1200 1210 1220 1230 1240 1250 1260

gtgctgcaaaatagcaaagaagaagctttaaacaatgcatttaaggggatgacaatactggagaaaataacatcgtccaagaactgaca

V L Q N S K E E A L N N A F K G D D N T G E N N I V Q E L T

1270 1280 1290 1300 1310 1320 1330 1340 1350

aaggagatcatctcagaagtgcagaggatgacgggcaatgacgtctgctgtgactgtggggcgccagatcctacatggctttccaccaac

K E I I S E V Q R M T G N D V C C D C G A P D P T W L S T N

ARF GAP

1360 1370 1380 1390 1400 1410 1420 1430 1440

ctgggcatcctgacctgcatcgagtgttccggaatccaccgagagctgggggttcattattccaggatgcagtccctgaccttagatgta

L G I L T C I E C S G I H R E L G V H Y S R M Q S L T L D V

1450 1460 1470 1480 1490 1500 1510 1520 1530

ctgggaacatctgagctgctgctcgccaagaatattgggaatgcaggctttaatgagatcatggaatgttgcctaccagctgaggactca

L G T S E L L L A K N I G N A G F N E I M E C C L P A E D S

1540 1550 1560 1570 1580 1590 1600 1610 1620

gtcaaacccaacccaggcagcgacatgaatgcaagaaaggactacatcacagccaagtacatcgagaggagatacgcaaggaagaagcac

V K P N P G S D M N A R K D Y I T A K Y I E R R Y A R K K H

1630 1640 1650 1660 1670 1680 1690 1700 1710

gcggataacgcggcgaagcttcacagtctttgcgaggccgtcaaaacgagagatatttttggattgctccaagcttatgctgatggtgtg

A D N A A K L H S L C E A V K T R D I F G L L Q A Y A D G V

1720 1730 1740 1750 1760 1770 1780 1790 1800

gatcttacggaaaaaatcccactggccaacggacatgagccggatgaaacggccctccaccttgcagtcagatccgtggatcgaacctct

D L T E K I P L A N G H E P D E T A L H L A V R S V D R T S

1810 1820 1830 1840 1850 1860 1870 1880 1890

cttcacattgtagacttttagttcagaacagtgggaacctggataaacagacagggaaaggcagcacagccctgcactactgctgcctg

L H I V D F L V Q N S G N L D K Q T G K G S T A L H Y C C L

1900 1910 1920 1930 1940 1950 1960 1970 1980

accgacaatgccgagtgcctcaagttgctcctgcgggggaaggcctccatcgagatagcaaacgagtcaggagagactccgctggacatt

ANKs

T D N A E C L K L L L R G K A S I E I A N E S G E T P L D I

1990 2000 2010 2020 2030 2040 2050 2060 2070

gccaagcgcctcaagcacgagcactgtgaggagctgctgacccaagccttatctggaagatttaattctcacgttcacgttgaatatgaa

A K R L K H E H C E E L L T Q A L S G R F N S H V H V E Y E

2080 2090 2100 2110 2120 2130 2140 2150 2160

tggcgactactccacgaagacctggatgaaagtgatgacgacatggatgagaaattgcagcccagtcccaaccggcgggaagaccggccc

W R L L H E D L D E S D D D M D E K L Q P S P N R R E D R P

2170 2180 2190 2200 2210 2220 2230 2240 2250

atcagcttctaccagctgggctccaaccagcttcagtctaacgctgtatctttggccagagatgctgcaaaccttgccaaggagaagcag

I S F Y Q L G S N Q L Q S N A V S L A R D A A N L A K E K Q

2260 2270 2280 2290 2300 2310 2320 2330 2340

agggctttcatgcccagcatcttgcagaatgagacttacggagccctcctgagtggcagcccacctcccgcccagcctgcagcccccagc

R A F M P S I L Q N E T Y G A L L S G S P P P A Q P A A P S

Pro-rich

2350 2360 2370 2380 2390 2400 2410 2420 2430

accaccagcgcccccccgcttcctccacggaatgttggcaaagttcagacagcctcctctgctaacaccctgtggaagacaaactctgta

T T S A P P L P P R N V G K V Q T A S S A N T L W K T N S V

2440 2450 2460 2470 2480 2490 2500 2510 2520

agtgtggacggtggaagccggcagcgatcttcgtcagatccgccagctgtccatccaccgctgccccctcttcgcgtgacatctaccaat

S V D G G S R Q R S S S D P P A V H P P L P P L R V T S T N

2530 2540 2550 2560 2570 2580 2590 2600 2610

cccctgacccccacgccgcccccacccgttgccaagacgcccagcgtaatggaagccttgagccagccgagcaagcctgccccgcctggg

P L T P T P P P P V A K T P S V M E A L S Q P S K P A P P G

2620 2630 2640 2650 2660 2670 2680 2690 2700

atctcacagatcaggcccccacctctgcccccacagccgcccagccgcctcccgcagaagaagcctgcgccgggggctgacaagtccacc

I S Q I R P P P L P P Q P P S R L P Q K K P A P G A D K S T

2710 2720 2730 2740 2750 2760 2770 2780 2790

ccactgaccaacaaaggccaaccgagaggacctgtggatctctctgcaacggaagctctgggtcctctgtccaatgctatggtcctgcag

P L T N K G Q P R G P V D L S A T E A L G P L S N A M V L Q

2800 2810 2820 2830 2840 2850 2860 2870 2880

ccccctgcacccatgcctaggaagtcgcaggcaaccaagttgaagcctaagcgggtgaaagcgctctataactgtgtggctgacaacccc

P P A P M P R K S Q A T K L K P K R V K A L Y N C V A D N P

2890 2900 2910 2920 2930 2940 2950 2960 2970

gatgagctcaccttctccgaggggggatgtgatcatcgtggacggggaggaggaccaggagtggtggattggccacattgatggagatcct

D E L T F S E G D V I I V D G E E D Q E W W I G H I D G D P

SH3

2980 2990 3000 3010 3020 3030

ggtcgcaaaggcgcattcccggtgtcatttgtgcactttatcgctgactga

G R K G A F P V S F V H F I A D *

Figure 6 Primary structure of PAG3. The numbers represent positions of the nucleotide, where the A at the first ATG is numer 1. The PH domain, ARFGAP domain , ankyrin repeats (ANKs), proline-rich (Pro-rich) and SH3 are overlined with gray, green, pink and yellow, respectively. The zinc finger motif (CxxC-x16-CxxC, where x is any amino acid) of the ARFGAP domain is underlined with a double line.

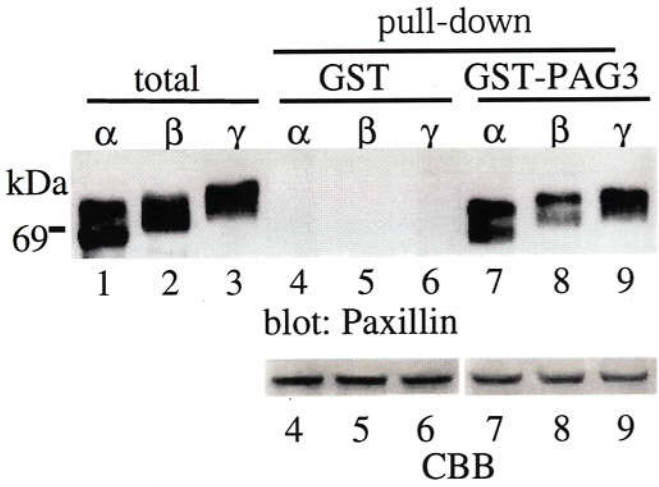

Figure 7 PAG3 binding to paxillin isoforms. Each 2.5 μg of GST alone (lane 4-6) or a GST-fusion form of PAG3 (lane 7-9) expressed in COS-7 cells and purified on glutathione-beads were incubated with 15 μg of Sf-9 cell lysates each producing recombinant paxillin isoforms of α, β and γ. After incubation, beads were washed and proteins retained on the beads were subjected to immunoblotting analysis using anti-paxillin antibody, Ab 199-217. Each 0.5 μg of the same cell lysates included as "total" (lane 1-3) In panel, amounts of each fusion protein used for pull-down assays are shown by the coomassie staining (CBB).

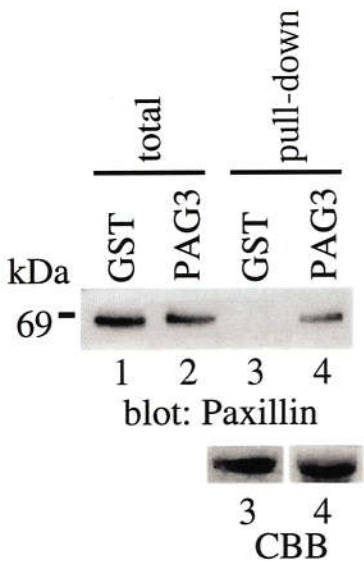

Figure 8 Association of PAG3 and paxillin in vivo. 1 X 106 COS-7 cells were transfected with 10 μg pEBG or EBG/PAG3 plasmid, and GST (lane 3) or GST-PAG3 (lane 4) was pulled-down from each 1 mg of the cell lysate using glutathione-beads to analyze its association with endogenous paxillin. Each 30 μg of the total cell lysates was included in lane 1 (cells with pEBG) and lane 2 (cells with pEBG/PAG3). Immunoblot was done with anti-paxillin antibody, Ab199-217. In panel, amounts of each fusion protein used for pull-down assays are shown by the coomassie staining (CBB).

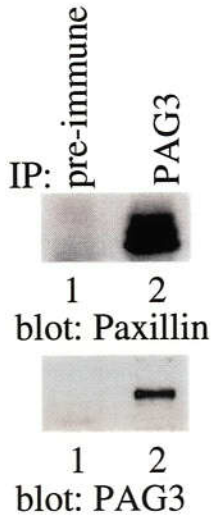

Figure 9 In vivo association of endogenous PAG3 and paxillin. Each 1 mg of cell lysate prepared from TPA-treated U937 cells were subjected to immunoprecipitation using anti-PAG3 antibody (lane2) or the pre-immune serum (lane1) coupled with protein A-Sepharose beads. Precipitated proteins were then subjected to immunoblotting analyzing anti-paxillin antibody, Ab199-217, and anti-PAG3 antibody.

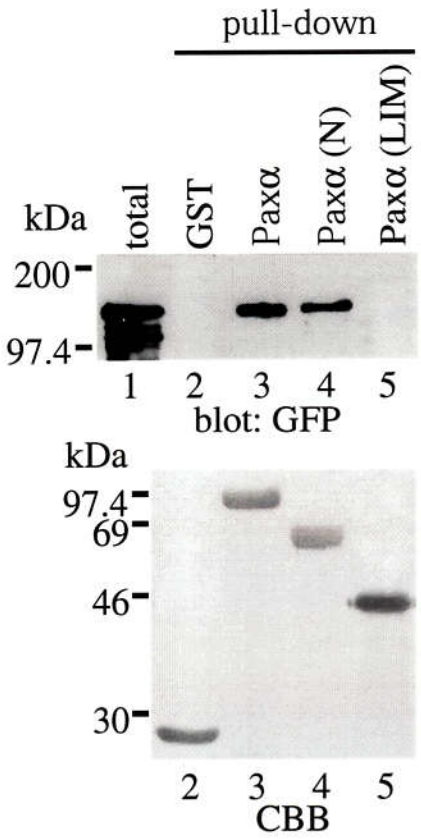

Figure 10 PAG3 binds to the N-terminal region of paxillin. Each 5 μg of GST alone (lane 2) GST-fusion forms of paxillin wild type and mutants (lane 3-5) as described in Materials and Methods were purified on glutathione-beads, and incubated with 500 μg of COS-7 cell lysate expressing EGFP-fusion forms of PAG3 to test binding. 30 μg of the total COS-7 cell lysate was included in lane 1. Immunoblot was done with anti-GFP antibody. In panel, amounts of each fusion protein used for pull-down assays are shown by the coomassie staining (CBB).

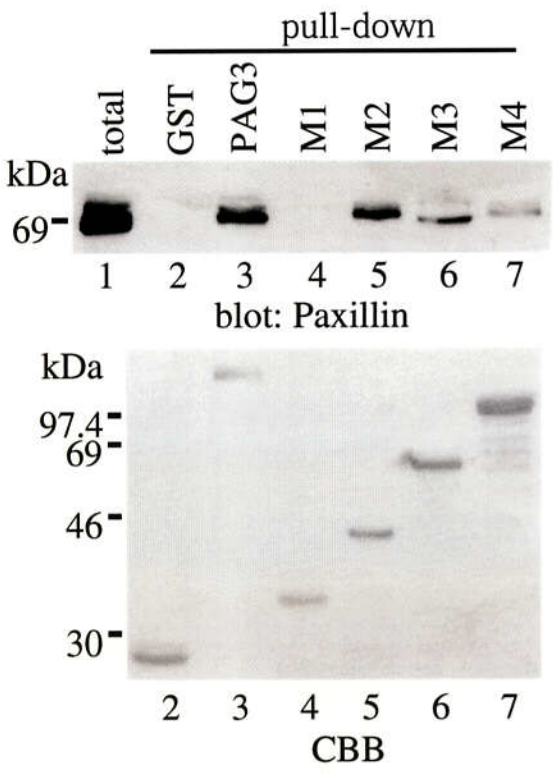

Figure 11 Paxillin binds to the C-terminal region of PAG3. Each 2.5 μg of GST alone (lane 2) or GST-fusion forms of wild type and deletion mutants of PAG3 (lane 3-7) purified on glutathione-beads as described in Material and Methods were incubated with 15 μg of Sf-9 cell lysate producing recombinant paxillin α to test binding.0.5 μg of the same cell lysate was included in lane 1. For the deletion mutants of M1-M4, see Fig. 1. In panel, amounts of each fusion protein used for pull-down assays are shown by the coomassie staining (CBB).

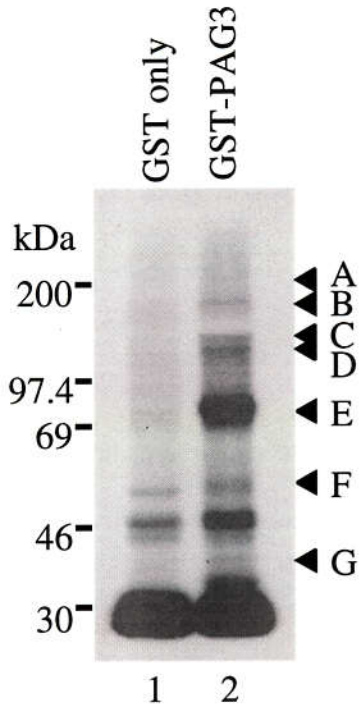

Figure 12 Protein bindings to PAG3 in vitro. Cell lysates prepared from1 x 107 radiolabeled HeLa cells were incubated with GST-PAG3, and bound proteins were separated by SDS-PAGE as described in materials and Methods. A negative control was included by incubating cell lysates with GST protein (lane 1). The resulting fluorograph is shown with exposure of 4 days at -80℃. Positions of protein bands (A-G) bound to GST-PAG3 over the negative control GST protein are shown on the right.

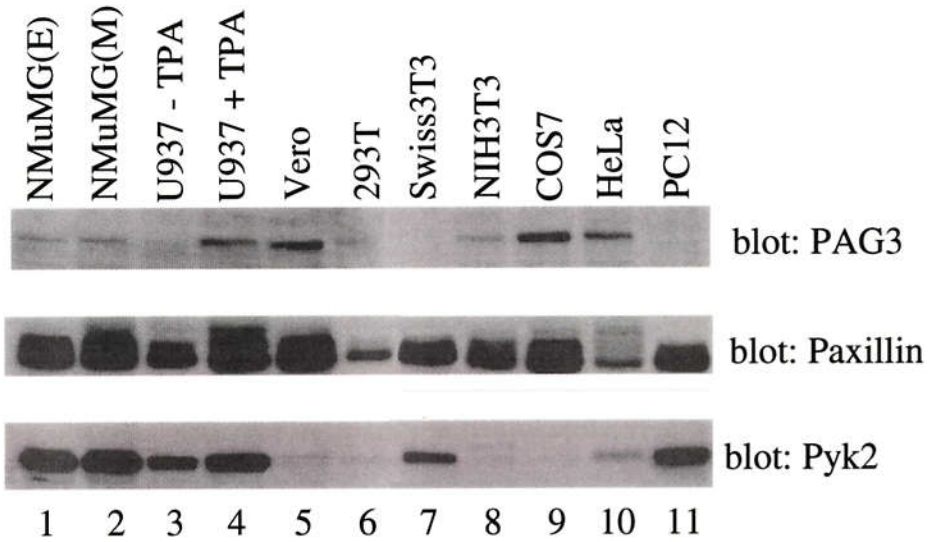

Figure 13 Cell lysates from several other cell lines were separated on SDS-PAGE and subjected to immunoblot analysis using anti-PAG3 antibody, anti-paxillin antibody (Ab199-217, Pax) and anti-Pyk2 antibody (Pyk2). NMuMG (E) shows epiterium-like cells and NMuMG (M) shows mesenchyme-like cells defferentiated by treatment with TGFβ for 2 days. Monocytes cells undifferentiated (-TPA) or differentiated by treatment with TPA for three days (+ TPA) are shown.

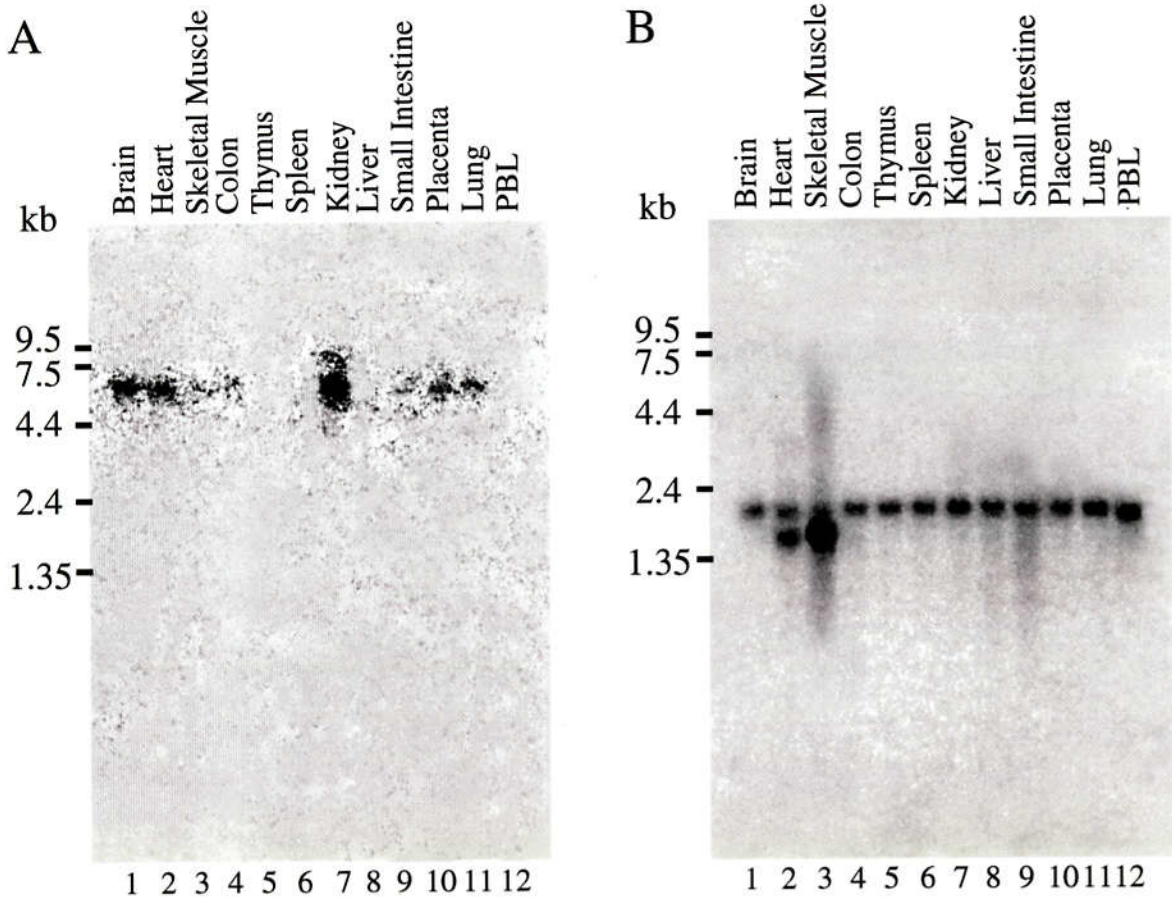

Figure 14 PAG3 mRNA expression in human tissues. Human multiple tissues for Northern blotting (Clontech) were probed with radiolabelled PAG3 cDNA fragment as described in Materials and Methods (A). Same filter blotted with β-actin probe was included as a control (B). Sizes in kilobases are shown on the rights. Exposure times were 3h for A, 2h for B; and radioactivities were detected using BAS2000 (Fuji Film). PBL, Peripheral Blood Leukocytes.

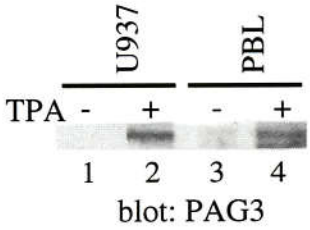

Figure 15 Induction of PAG3 in normal monocytes prepared from human peripheral blood (PBL). Cell lysates were prepared and subjected to immunoblot analysis using anti-PAG3 antibody, as in Fig. 10. Fresh monocytes were prepared and treated or untreated with TPA as described in Materials and Methods.

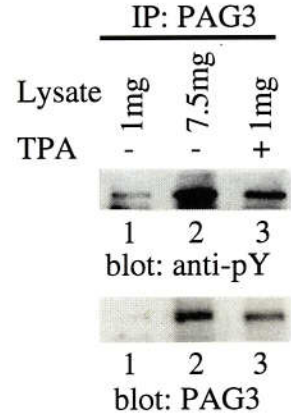

Figure 16 PAG3 protein was immunoprecipitated from U937 cells treated with or without TPA, and subjected to sequential immunoblot analysis using anti-phosphotyrosine antibody (4G10; anti-pY), and anti-PAG3 antibody.

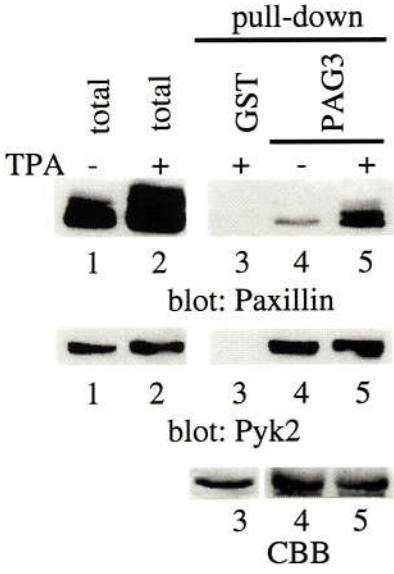

Figure 17 Cell lysates from TPA-treated or untreated U937 cells were incubated with GST-PAG3 purified on glutathione-beads to analyze PAG3 binding towards paxillin and Pyk2. Immunoblots were done with same membrane filter by sequential hybridization with anti-paxillin antibody (Ab199-217, Pax) and anti-Pyk2 antibody (Pyk2). In panel, amounts of each fusion protein used for pull-down assays are shown by the coomassie staining (CBB).

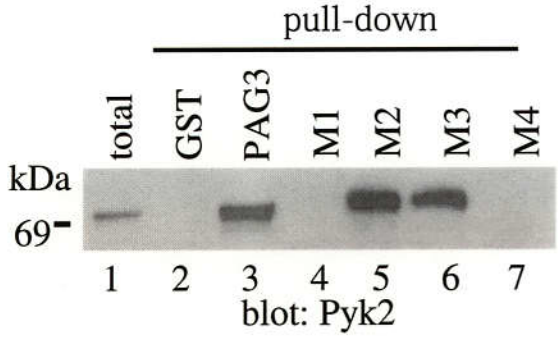

Figure 18 Pyk2 binds to the C-terminal region of PAG3. Each 5 μg of GST alone (lane 2) or GST-fusion forms of wild type PAG3 and its deletion mutants (lane 3-7) purified on glutathione-beads were incubated with each 6.5 mg of U937 cell lysate to test binding, as described in Material and Methods. 30 μg of the total cell lysate was included in lane 1. Blot was done with anti-Pyk2 antibody. For the deletion mutants of the M1-M4, see Fig. 1.

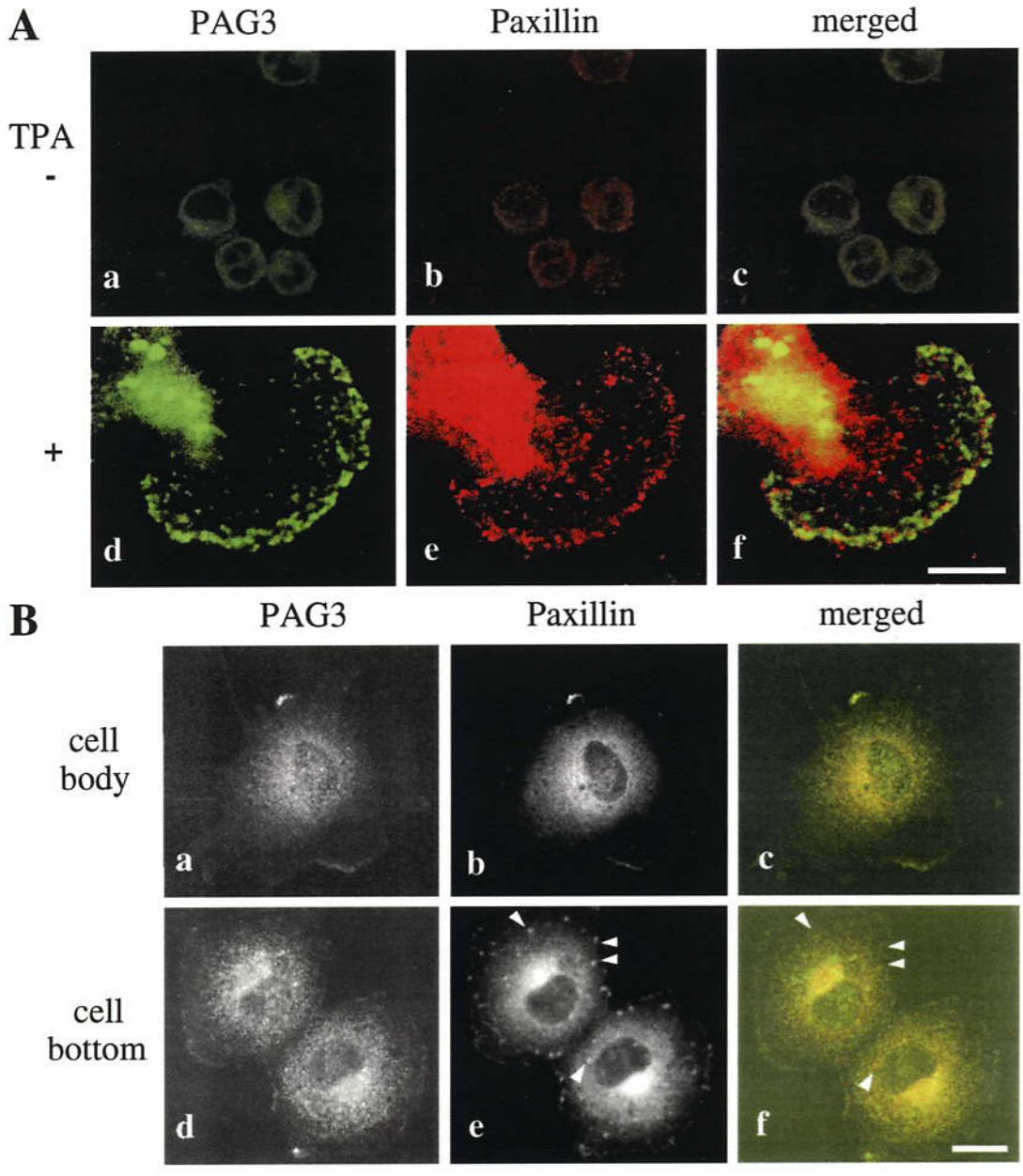

Figure 19 Colocalization of endogenous PAG3 and paxillin in the cytoplasm and at the cell periphery in U937 monocyte cells (A) and COS-7 epithelial cells (B). U937 monocyte cells undifferentiated (A, a-c) or differentiated by TPA treatment for three days (A, d-f) are shown. Cells fixed with 3.7% paraformaldehyde were double immunolabeled with rabbit polyclonal anti-PAG3 antibody (a and d) and mouse monoclonal anti-paxillin antibody (b and e), followed by Cy2-conjugated donkey anti-rabbit IgG and Cy5-conjugated donkey anti-mouse IgG, and examined by confocal laser scanning microscope. Focuses were adjusted 5.0 μm above the surface of the glass chamber plate in A (a-c) and 3.0 μm above this in B (a-c), each across the center of the nucleus in the majority of the cells; or 0.5 μm above this in A (d-f) and B (d-f), which are near to the bottom layers of cells. In e in B, paxillin localized at the cytoplasmic pool is still seen in addition to that localized to focal adhesion plaques, and several focal adhesion plaques are marked by arrow heads. The right column represents the merging of the left and the middle images. For clearer images of PAG3 and paxillin distribution, some photographs in B (a, b, d and e) are shown as black and white images. Bars, 20 μm.

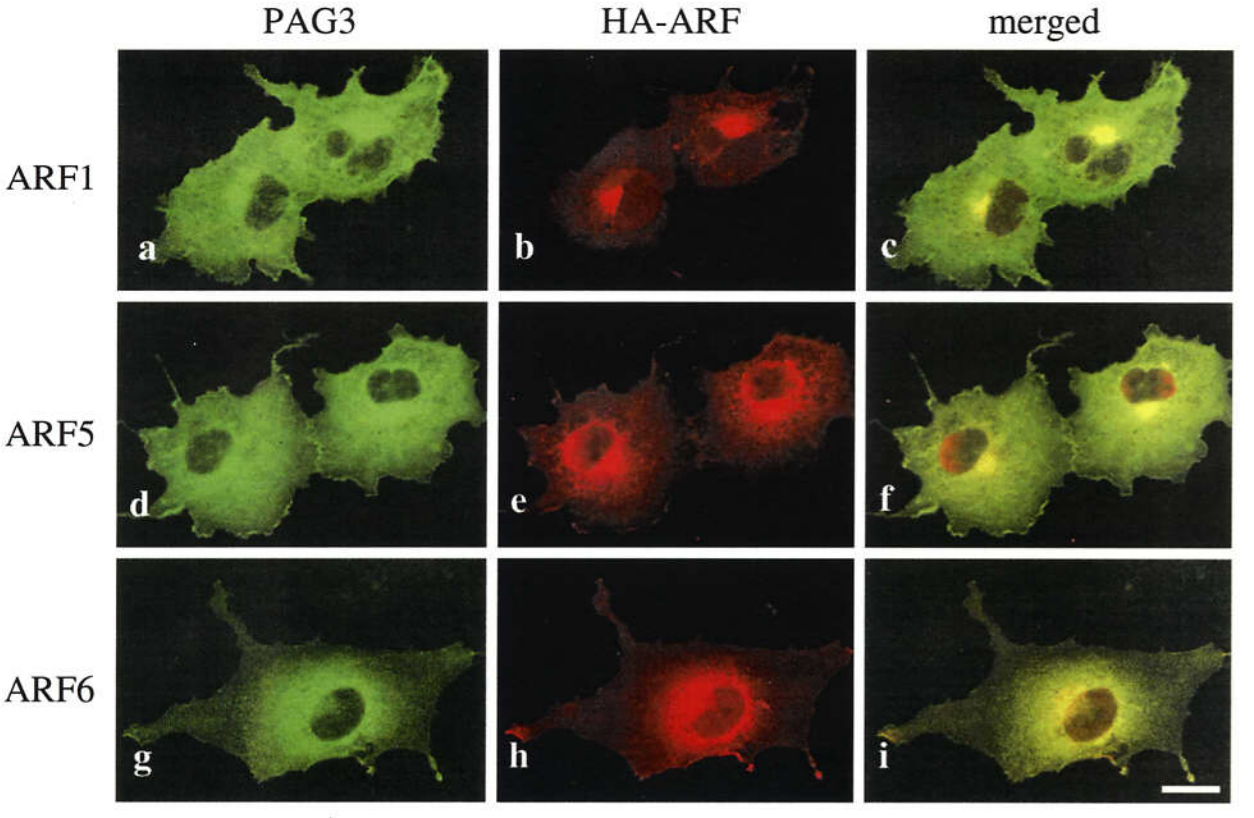

Figure 20. PAG3 and ARF isoforms. Subcellular localization of PAG3 overlap with those of ARF1, ARF5 and ARF6; but colocalization with PAG3 is more readily observed for ARF5 and ARF6, rather than for ARF1. COS-7 cells were transiently transfected by the calcium precipitation method with each plasmid encoding either one of HA-tagged wild type ARF isoforms (a-c, ARF1; d-f, ARF5; g-i, ARF6), then fixed and each ARF protein was visualized by immunolabeling for the HA epitope using mouse monoclonal anti-HA antibody and Cy5-conjugated donkey anti-mouse antibody (b, e and h). Endogenous PAG3 was visualized by anti-PAG3 antibody and Cy2-conjugated donkey anti-rabbit antibody (a, d and g). Focuses were adjusted 3.0 μm above the surface of the glass chamber plate, across the center of the nucleus in the majority of the cells, and the each right column represents the merging of the left and the middle images. Bar, 20 μm.

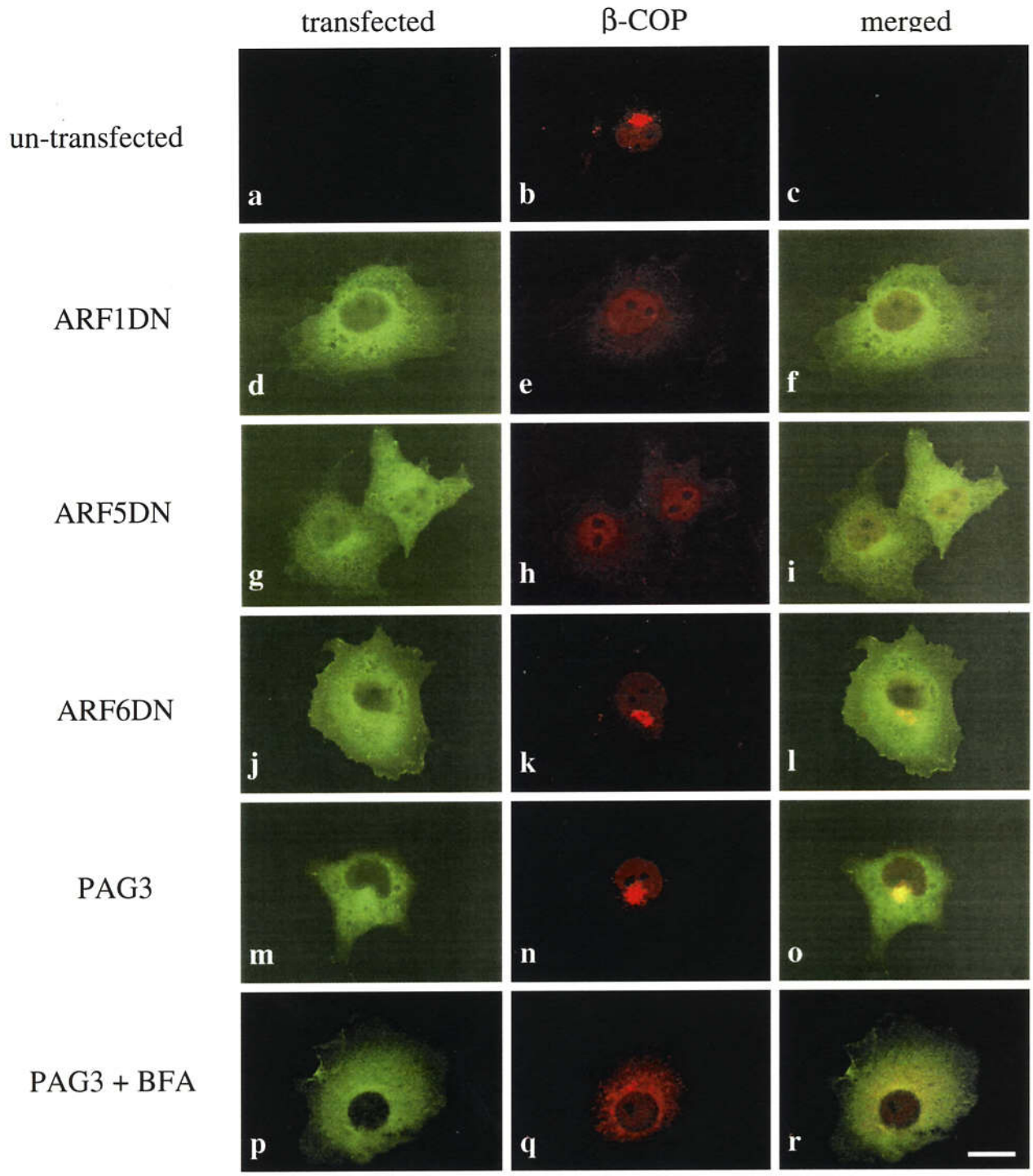

Figure 21 Overexpression of PAG3 does not affect the subcellular distribution of β-COP. COS-7 cells were transiently transfected by calcium precipitation method with plasmids encoding either one of HA-tagged DN forms of ARF isoforms (ARF1N126I, ARF5N126I, and ARF6N122I) or EGFP-tagged PAG3. Cells were then fixed and double immunolabeled for HA epitope and endogenous β-COP using mouse anti-HA antibody and rabbit anti-β-COP antibody, followed by Cy2-conjugated anti-rabbit IgG and Cy5-conjugated anti-mouse antibody. PAG3 was detected by the fluorescence from the EGFP tag. Labelled cells were then visualized using confocal scanning laser microscope. Focuses were adjusted 3.0 μm above the surface fo the glass chamber plate. Each right column represents the merging of the left and the middle images.. Bar, 20 μm.

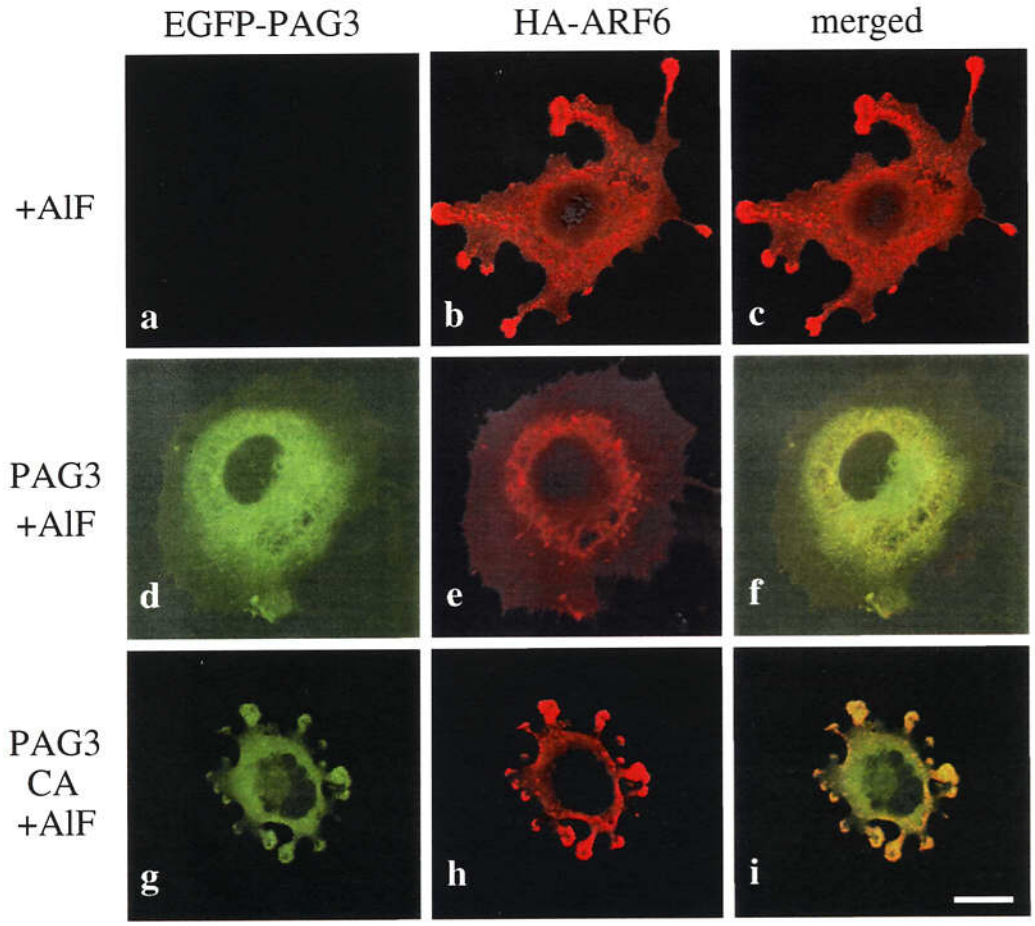

Figure 22 Possible functional interaction between PAG3 and ARF6. Overexpression of PAG3, but not its GAP-inactive mutant, counteracted ARF6 activity in the ARF6-transfected and the AlF treated cells. COS-7 cells were transiently transfected by FuGENE6 with plasmids encoding HA-tagged wild type ARF6 (a-c), or cotransfected with plasmids encoding HA-tagged wild type ARF6 and EGFP-tagged wild type (d-f) or with plasmids encoding HA-tagged wild type ARF6 and CA mutant of PAG3 (g-i). Each 0.5 μg of PAG3 and 0.5 μg of ARF plasmids were used, as determined by our preliminary titration experiments. Cells were then treated with AlF for 1 h at 37 ℃ as described in Materials and Methods, and fixed. PAG3 proteins were visualized by the fluorescence from the EGFP-tag (d and g). ARF6 (b, e and h) were visualized as in Fig. 17. Focuses were adjusted 3.0 μm above the surface of the glass chamber plate, across the center of the nucleus in the majority of the cells, and the each right column represents the merging of the left and the middle images. Bar, 20 μm.

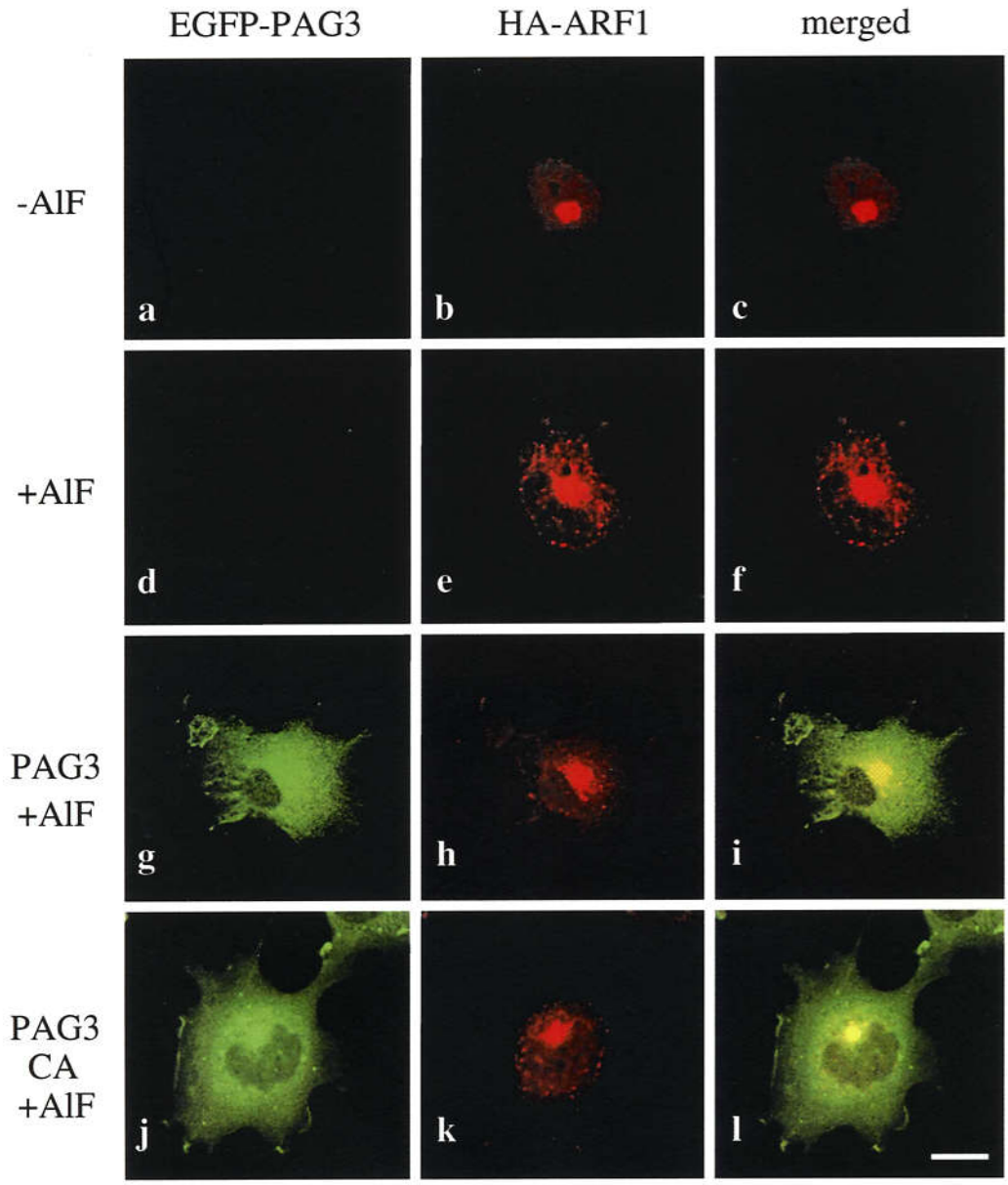

Figure 23 PAG3 does not counteracted ARF1 activity. COS-7 cells were transiently transfected by FuGENE6 with plasmids encoding HA-ARF1 (a-f), or cotransfected with plasmids encoding HA-ARF1 and EGFP-PAG3 (g-i), or with plasmids encoding HA-ARF1 and the CA mutant of EGFP-PAG3 (j-l). Each 0.5 μg of PAG3 and ARF plasmids were used, as determined by our preliminary titration experiments. Cells were then treated with AlF mixture for 1 h at 37 ^{o}C before fixation, as described in Materials and Methods. PAG3 proteins were visualized by the fluorescence from the EGFP-tag (g and j). ARF1 (b, e, h and k) were visualized by immunolabeling for the HA epitope using mouse anti-HA antibody and Cy5-conjugated anti-mouse antibody (b, e, h and k). Focuses were adjusted 3.0 μm above the surface of the glass chamber plate. Each right column represents the merging of the left and the middle images. Bar, 20 μm.

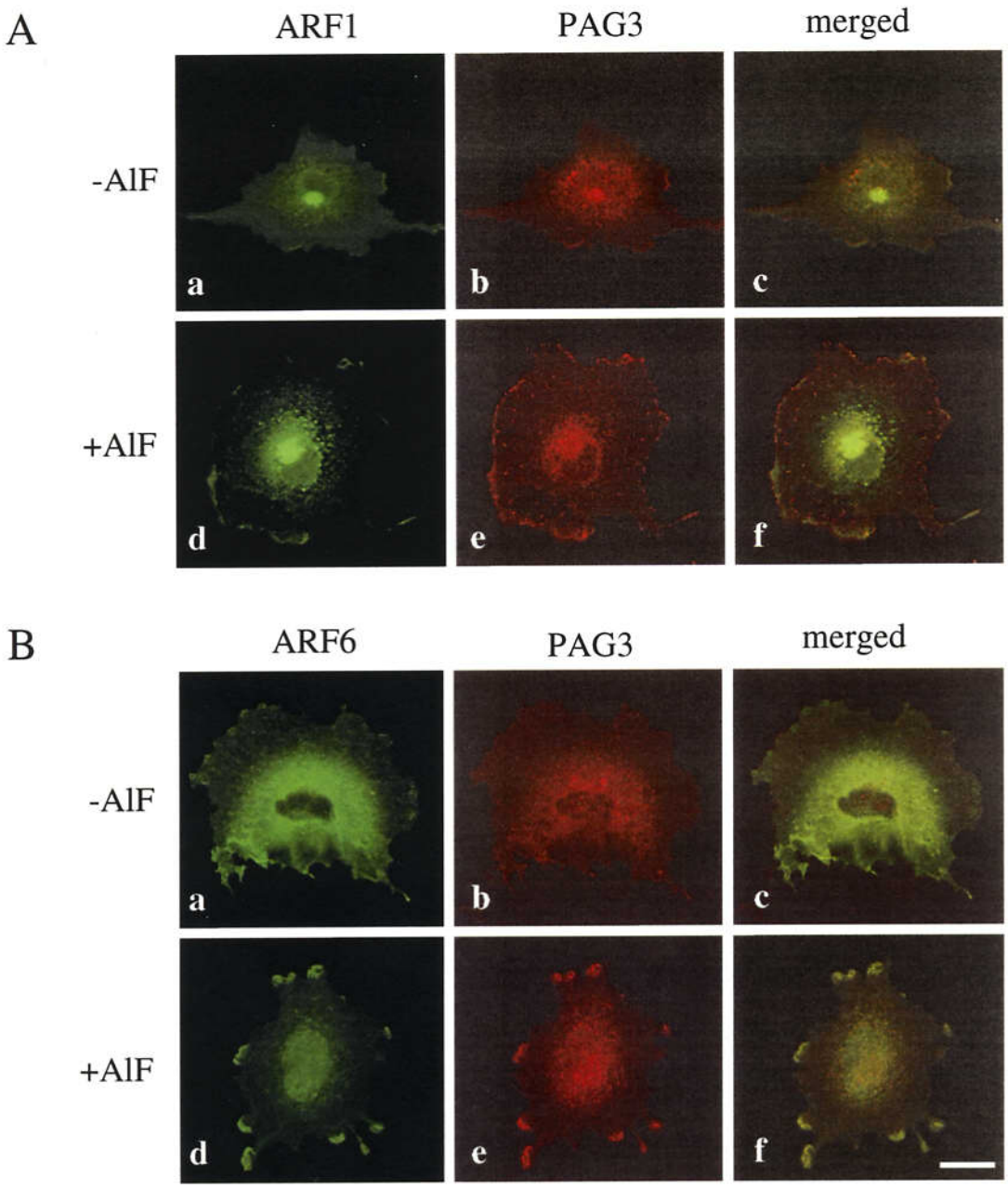

Figure 24 Subcellular localization of PAG3 is under the control of the ARF6 activity. COS-7 cells were transiently transfected by FuGENE6 with plasmids encoding HA-ARF1 (A; a-f), or HA-ARF6 (B; a-f). Each 1.0 μg of ARF plasmids were used. Cells (d-f, g-j) were treated with AlF for 1 h at 37 °C before fixation, as described in Materials and Methods. Endogenous PAG3 proteins were visualized by immunolabeling using rabbit anti-PAG3 antibody and Cy2-conjugated anti-rabbit antibody (b, e, h and k). ARF1 and ARF6 (a and d) were visualized as in Fig. 19 (a and in A and B). Focuses were adjusted 3.0 μm above the surface of the glass chamber plate. Each right column represents the merging of the left and the middle images. Bar, 20 μm.

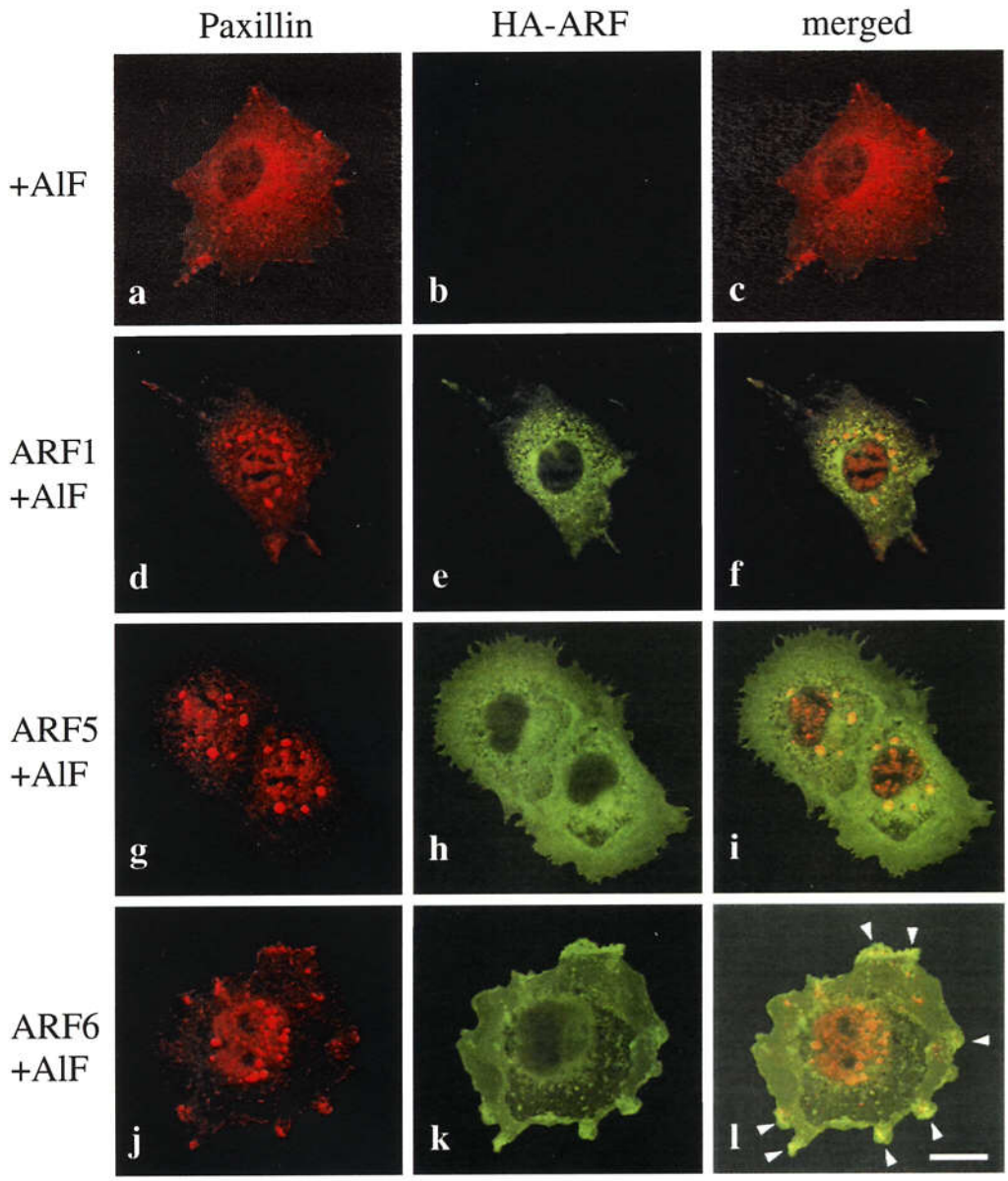

Figure 25 ARF activities affect subcellular localization of paxillin. COS-7 cells untransfected (a-c) or were transiently transfected by FuGENE 6 with each plasmid encoding either one of HA-tagged wild type ARF1 (d-f), ARF5 (g-h) or ARF6 (j-l), then treated with AlF for 1 h at 37 ^{o}C. Cells were then fixed and endogenous paxillin (a, d, g and j) were visualized using rabbit polyclonal anti-paxillin antibodies, coupled with Cy5-conjugated donkey anti-rabbit antibody; and HA-ARF proteins (e, h and k) were by mouse monoclonal anti-HA antibody, coupled with Cy2-conjugated donkey anti-mouse antibody. Focuses were adjusted 3.0 mm above the surface of the glass chamber plate. The right column represents the merging of the left and the middle images (c, f, i and l). Arrow heads in panel 1 indicate areas where paxillin is colocalized with ARF6. Bar, 20 μm. Expression of these wild type HA-ARF proteins in the absence of the AlF-treatment did not affect significantly the subcellular localization of paxillin (data not shown): see Fig. 18 (b in B) for the subcellular distribution of paxillin for the comparison.

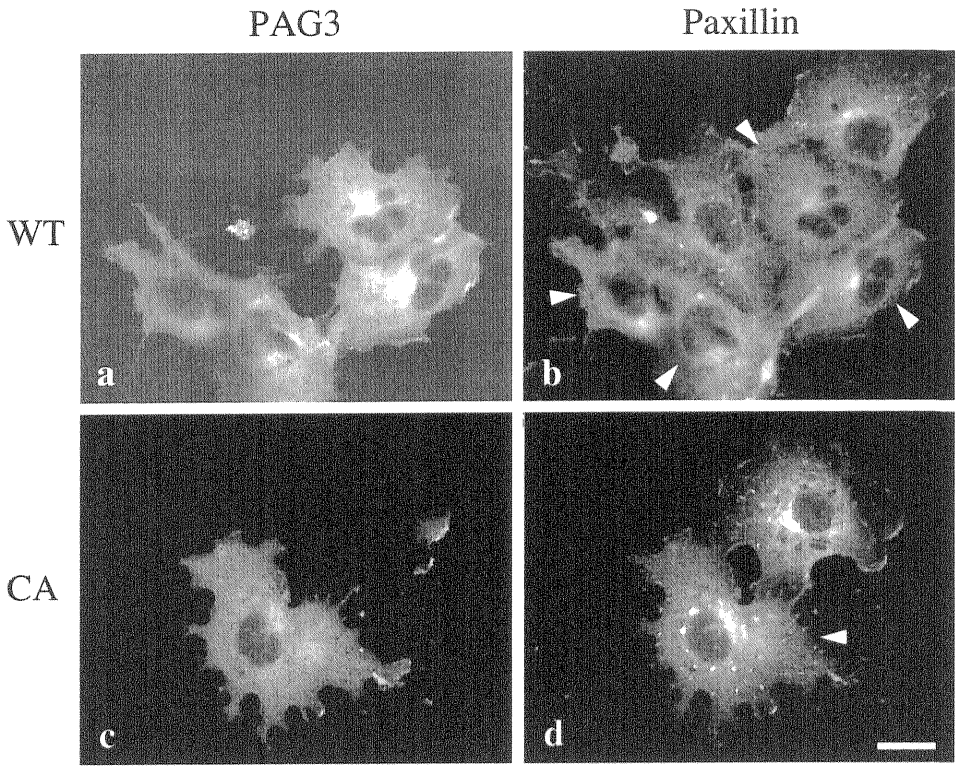

Figure 26 Overerxpression of PAG3, but not its GAP-inactive mutant, inhibits paxillin recruitment to focal contacts. COS-7 cells were transiently transfected by the calcium precipitation method with plasmids encoding EGFP-tagged PAG3 (a and b) or the CA mutant (c and d). Cell were then fixed and EGFP-PAG3 (a and c) and endogenous paxillin (b and d) were visualized as in Fig. 18 and Fig. 16, respectively. Focuses were adjusted 0.5 μm above the surface of the glass chamber plate, to visualize the focal contacts. The right column is of the same field as the left column and arrowheads indicate cells expressing EGFP-PAG3 proteins. Bar, 20 μm.

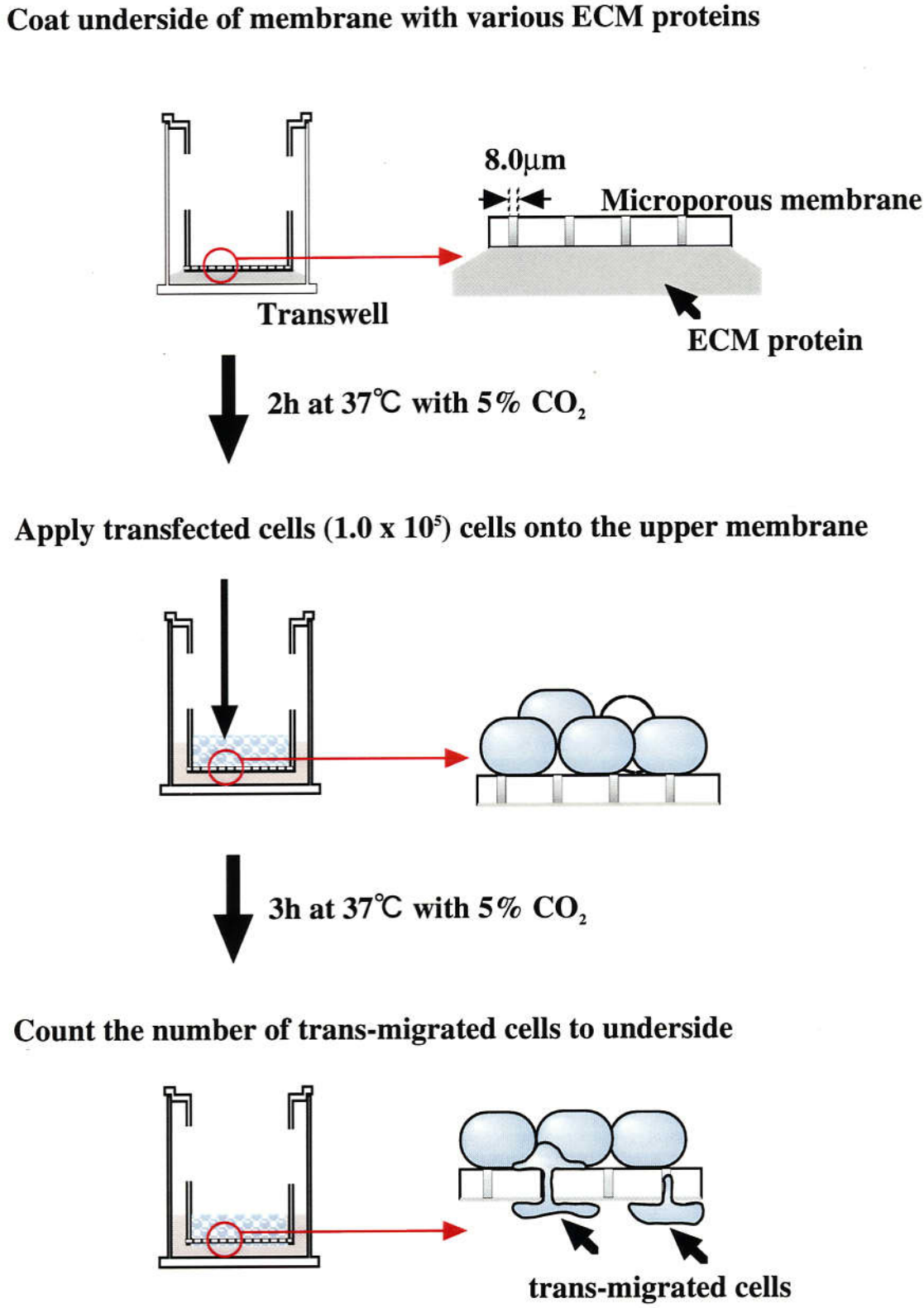

Figure 27 Haptotactic assay using modified boyden chamber was described in Material and Methods.

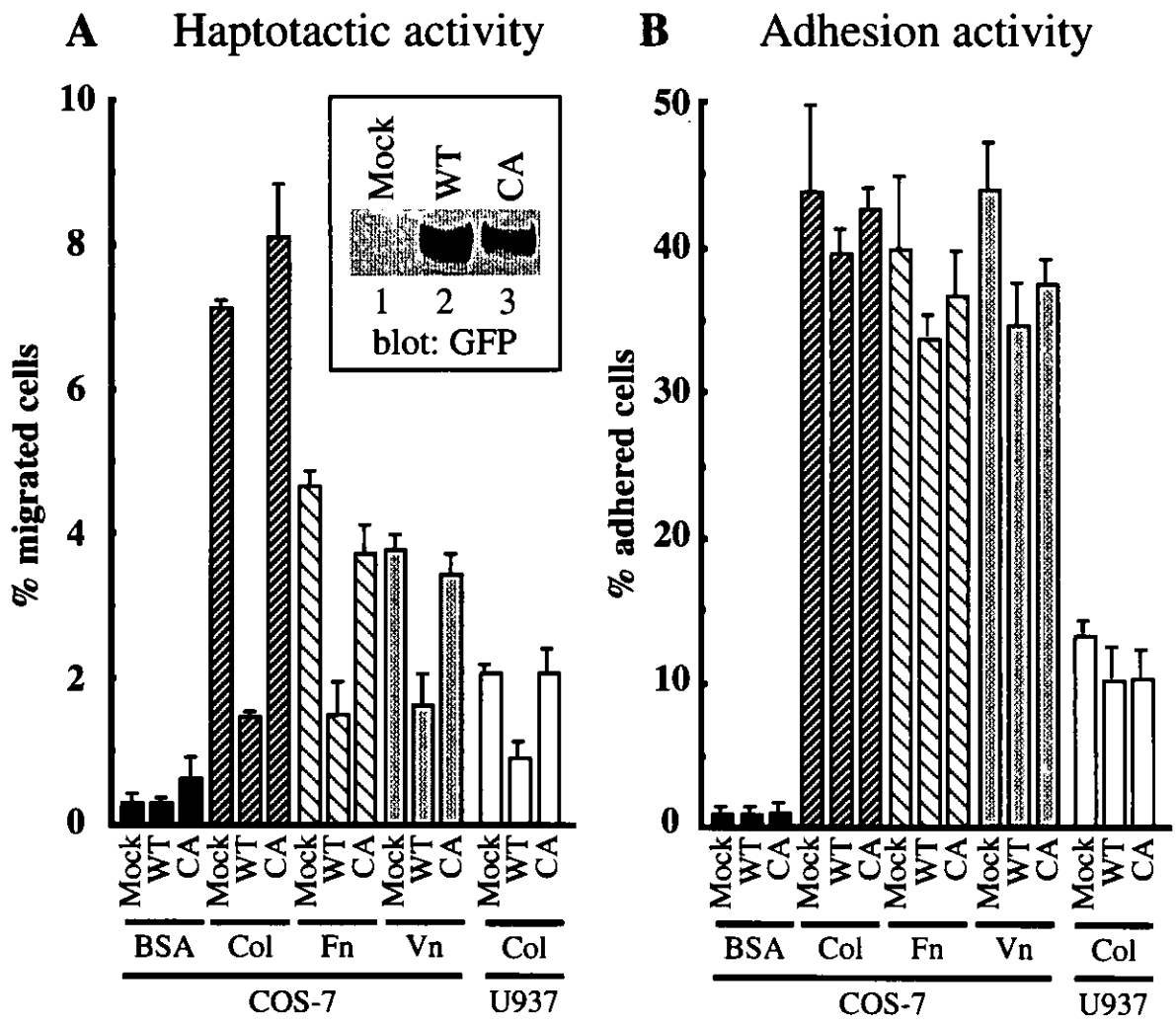

Figure 28 Overerxpression of PAG3, but not its GAP-inactive mutant, decreases the cell migratory activity without significant effect on the cell adhesive activity. COS-7 cells or U937 cells were transiently transfected with plasmids encoding EGFP-tagged PAG3 (WT) or the CA mutant (CA), or subjected to the transfection procedure without plasmid DNA (Mock). U937 cells were treated with TPA for three days. Cells were collected by trypsinization, and then subjected to adhesion assays or haptotaxis migration assays on collagen type I (Col), fibronectin (FN) or vitronectin (VN) in the absence of serum as described in Materials and Methods. BSA coating was used as a negative control. Transfected cells adhered 30 min after replating were enumerated by counting cells positive for the EGFP fluorescence, and cells migrating during 3 h were enumerated by counting cells on the underside of the membrane that were positive for the EGFP fluorescence. Percentages of cell adhesion and migration were calculated as described in Materials and Methods. Each bar represents the mean +/- SEM of triplicate experiments. Inset in panel A is the anti-GFP antibody immunoblot showing the expression levels of EGFP-tagged PAG3 (WT) or the CA mutant (CA) in COS-7 cells used in these experiments. Expression of EGFP-tagged PAG3 protein was then more than 10 - 20 times higher than that of endogenouse PAG3 (data not shown).

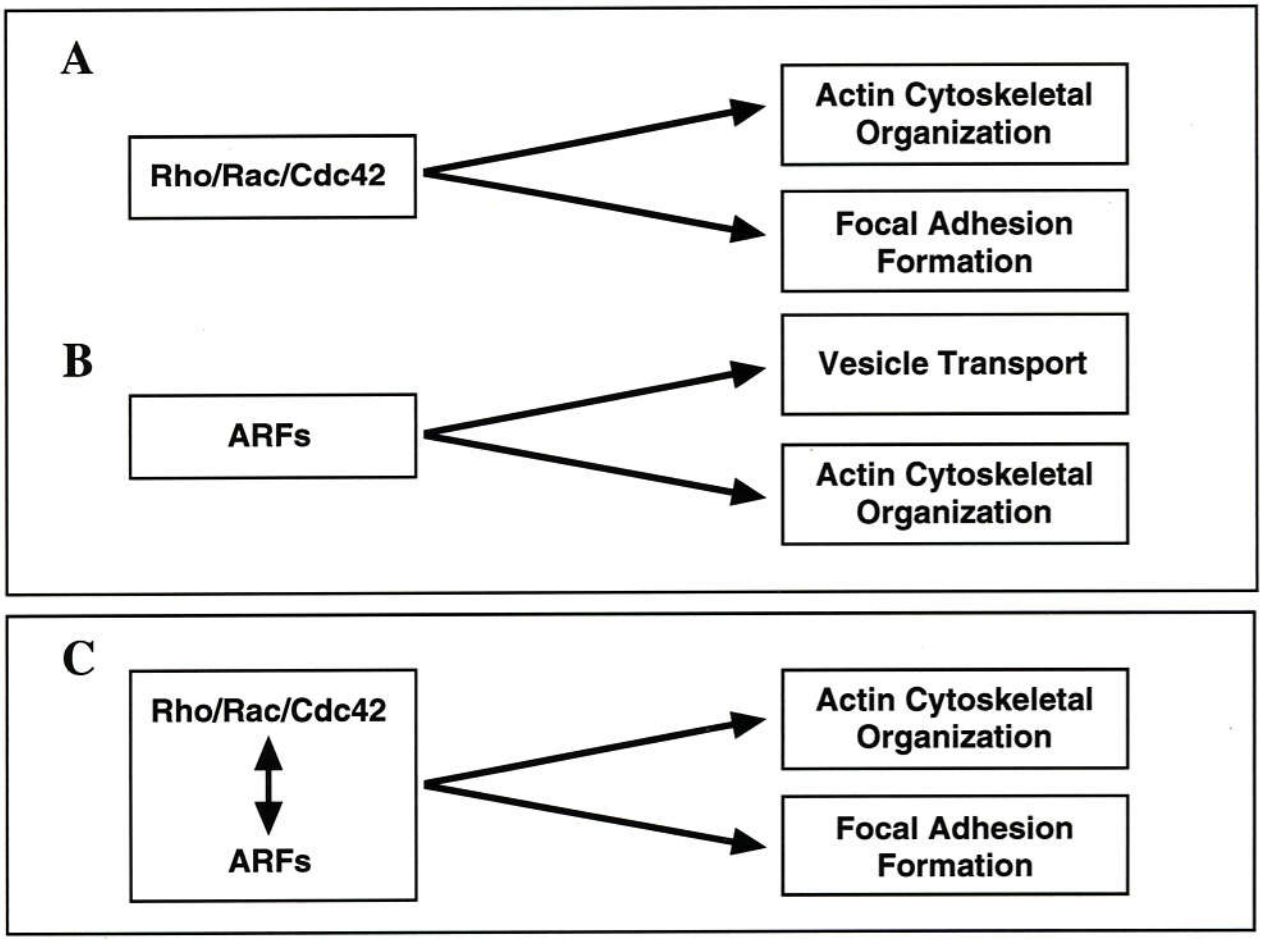

Figure 29 Haptotactic assay using modified boyden chamber was described in Material and Methods.

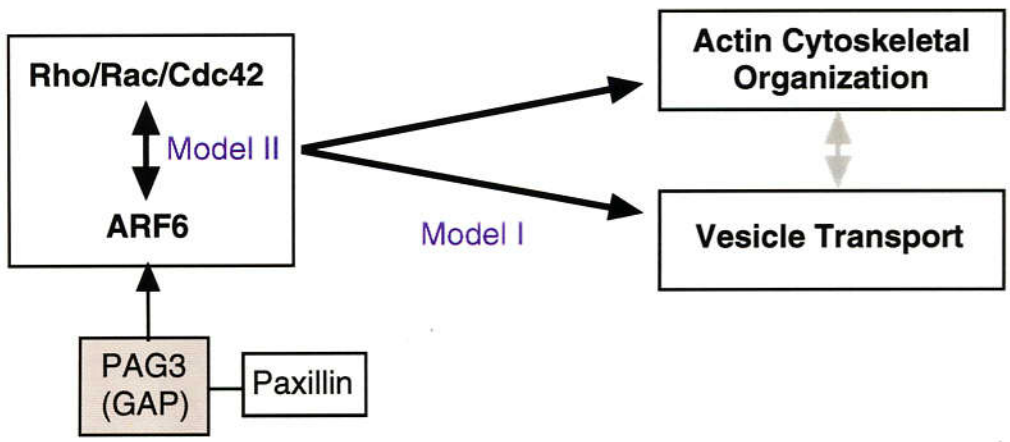

Figure 30 Hyphozesis of co-operation of Rho family, Arf6 and PAG3

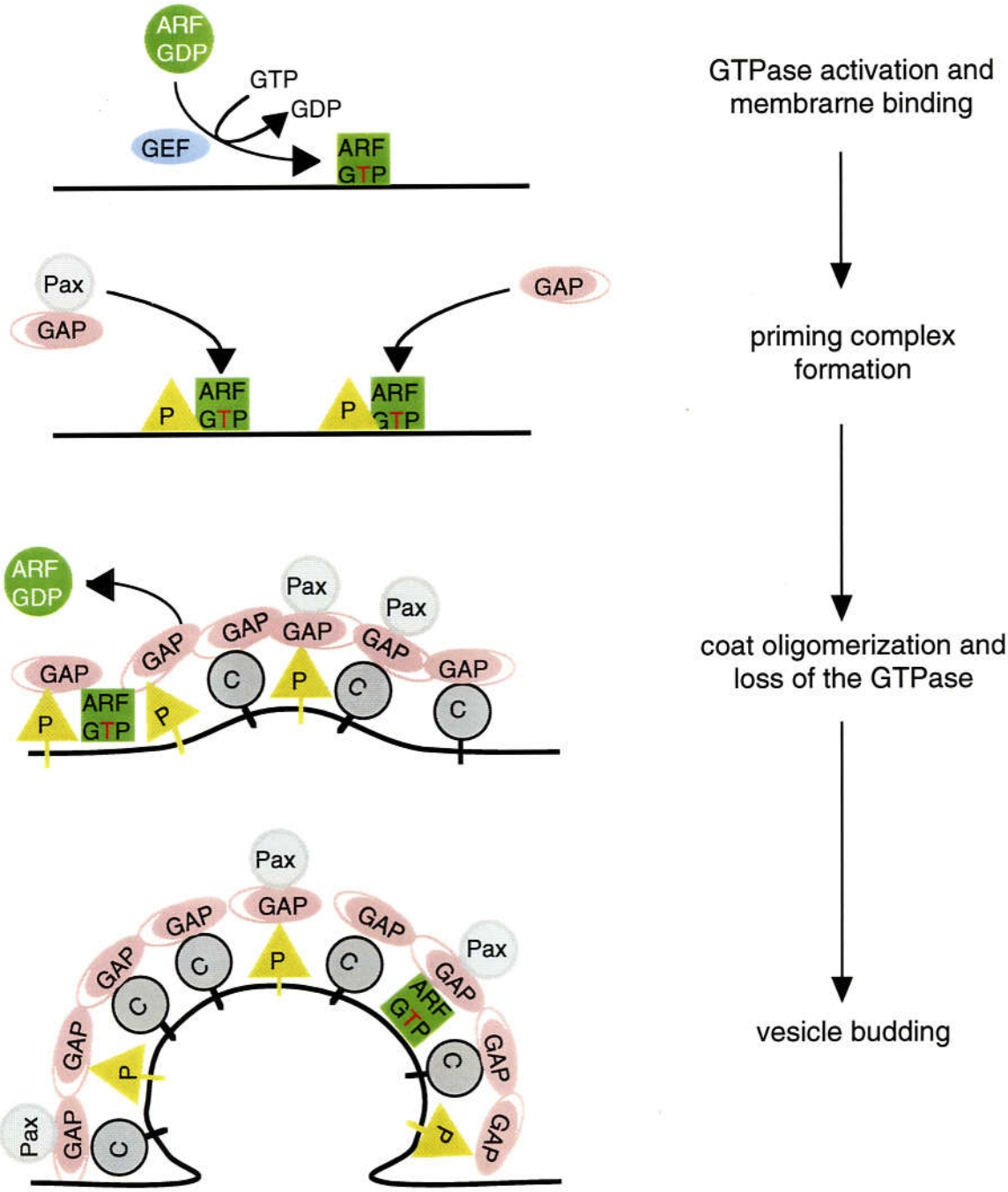

GEF : guanine nucleotide exchange factor

GAP : an coat component depicted as a dimer containing a GTPase-activating protein

C : Cargo proteins

P : a membrane protein that acts as a primer to form a priming complex.

ARFGDP :

ARFGTP :

Pax : Paxillin

Figure 31 Model I : Vesicle Transport
Reference : Springer, S. et al. Cell *97*

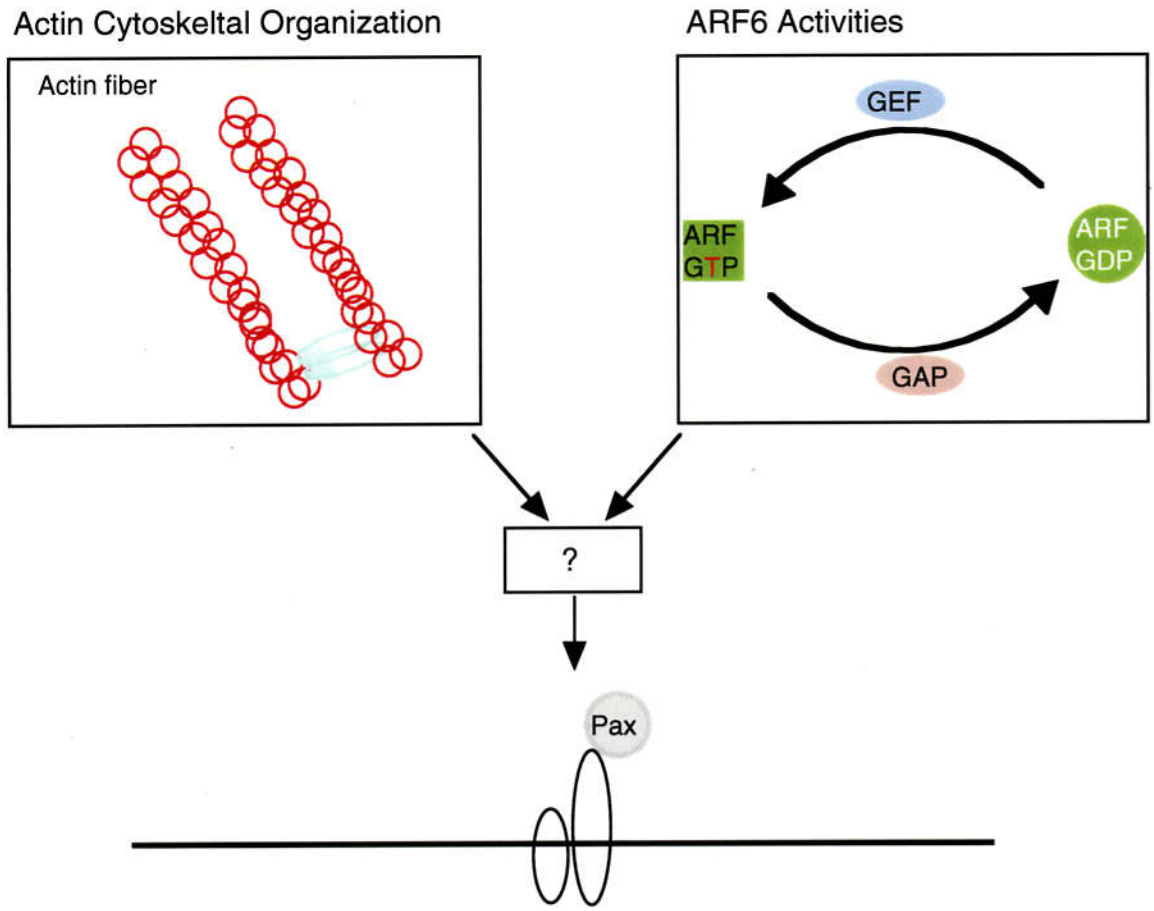

Figure 32 Model II : Actin Cytoskeletal Organization